



Weighing the Top with energy correlators

J. Holguin, I. Moult, A. Pathak, and M. Procura

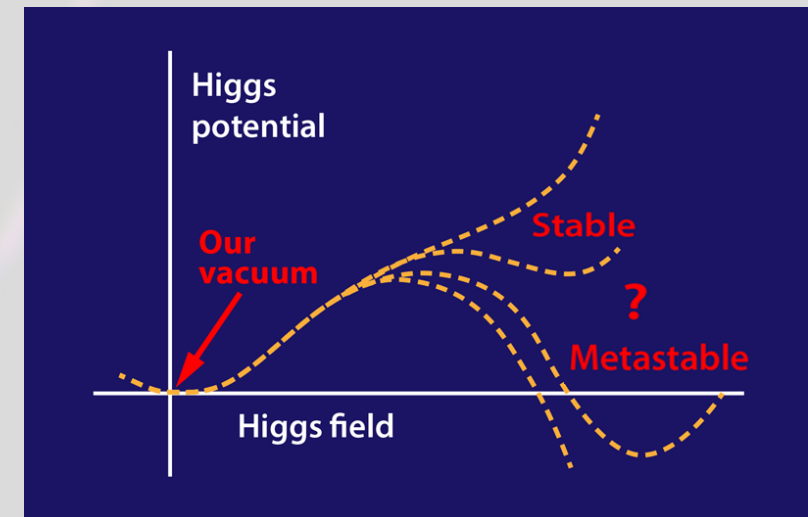
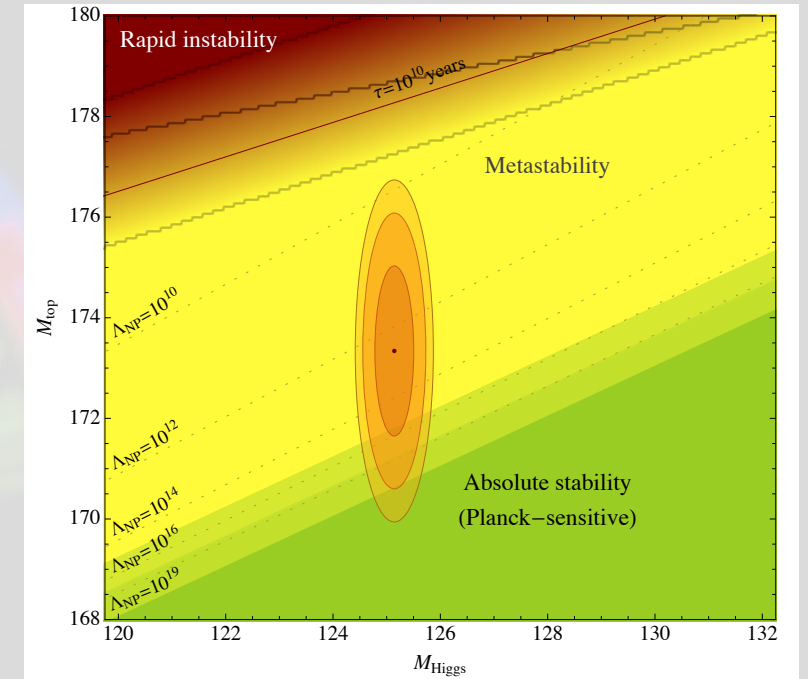
arXiv:2201.08393

cnrs



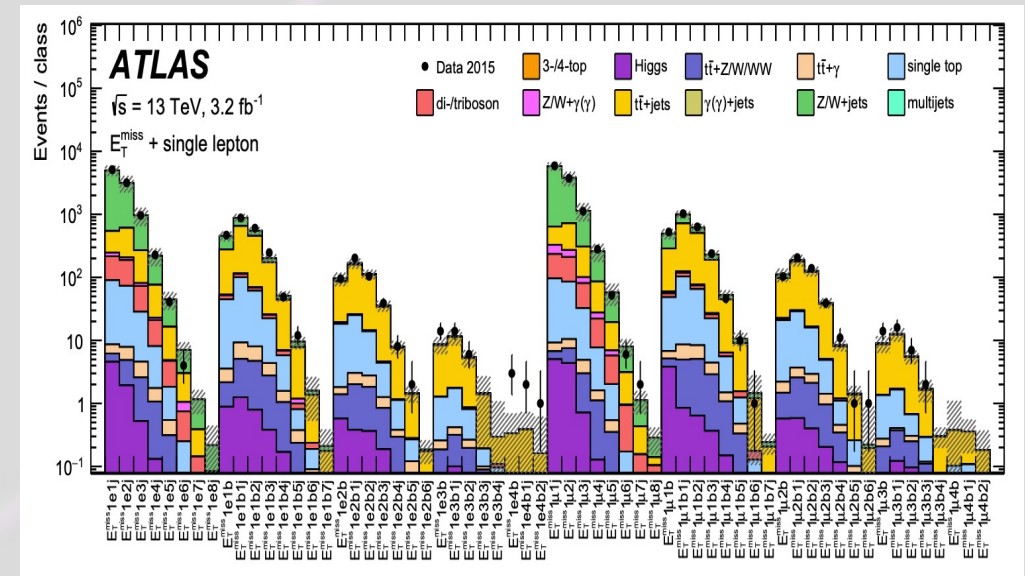
Why the top mass?

- The Top is very interesting!
 - Largest Yukawa coupling – sensitive to new physics.
 - The Top and the Higgs masses determine the stability of the electroweak vacuum. [1307.3536](#), [1408.0292](#)



Why the top mass?

- The Top is very interesting!
 - Largest Yukawa coupling – sensitive to new physics.
 - The Top and the Higgs masses determine the stability of the electroweak vacuum.
- We are in an unprecedented era of high statistics collider physics!
 - Top measurements have transitioned from discovery to precision.



Current status of top mass measurements

- Current world average (HL-LHC projection ~ 200 MeV)

- $m_t = 172.76 \pm 0.30$ GeV [10.1093/ptep/ptaa104](https://arxiv.org/abs/10.1093/ptep/ptaa104)

- An impressive uncertainty ~ 0.2 %!

- Some of the numbers that enter this world average:

- $m_t = 172.67 \pm 0.48$ GeV ATLAS, 1810.01772

- $m_t = 172.26 \pm 0.61$ GeV CMS, 1812.06489

- $m_t = 174.34 \pm 0.64$ GeV Tevatron, 1407.2682

- $m_t = 170.5 \pm 0.8$ GeV CMS, 1904.05237

The only quark with **three masses in PDG**:

Mass (direct measurements) $m = 172.76 \pm 0.30$ GeV ^[a,b] (S = 1.2)

Mass (from cross-section measurements) $m = 162.5^{+2.1}_{-1.5}$ GeV ^[a]

Mass (Pole from cross-section measurements) $m = 172.5 \pm 0.7$ GeV

How to measure the Top mass*

- What we have access to at a collider is a set of events and a (partial) kinematic breakdown of each event into particles with 4-momenta.
- Methods we might use:
 - Simplest: count the number of tagged top events to find $\sigma(m_t)$.
 - Slightly more sophisticated: measure a distribution differential in the event kinematics.
 - Best precision: direct measurement using Monte Carlo to simulate the top events and compare for a mass extraction.

*please allow me to oversimplify for a little bit

...but what is the Top mass we measure?

- The top quark mass is not a physical observable but a Lagrangian parameter,

$$\text{---} \xrightarrow{p} \text{---} + \text{---} \xrightarrow{p} \text{---} \text{---} + \dots \sim \frac{i}{\not{p} - m_t^0 - \Sigma(p, m_t^0, \mu)}$$

and must be renormalized in a definite *mass scheme*.

- We gain access to this parameter through a sensitive **physical observable**: $\sigma^{\text{exp}}(m_t^X, \Lambda_{\text{QCD}}, Y) = \sigma^{\text{pert}}(m_t^X, \alpha_s, Y, \dots) + \sigma^{\text{NP}}(\Lambda_{\text{QCD}}, Y, \dots)$

$$m_t^{\text{pole}} = m_t^X + \delta m_t^X$$

We will come back to this as it leads to complications!

How to measure the Top mass

- Can measure many different differential distributions.

$$\frac{d\sigma}{dm_t^{\text{reco}}}, \quad \frac{d\sigma}{dM_{bl}}, \quad \frac{d\sigma}{dM_{t\bar{t}}}, \quad \frac{d\sigma}{dM_{t\bar{t}j}}$$

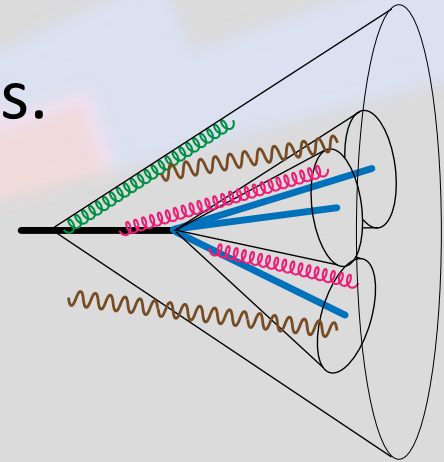
- These can be computed from theory

- Arguably best efforts for rigorous control over m_t use groomed jet masses: i.e.

$$(m_t)^2 = (\sum_i p_i)^2 \quad \text{0711.2079 and references therein} \quad m_t = 172.6 \pm 2.5 \text{ GeV} \quad \text{A recent measurement in CMS 1911.03800}$$

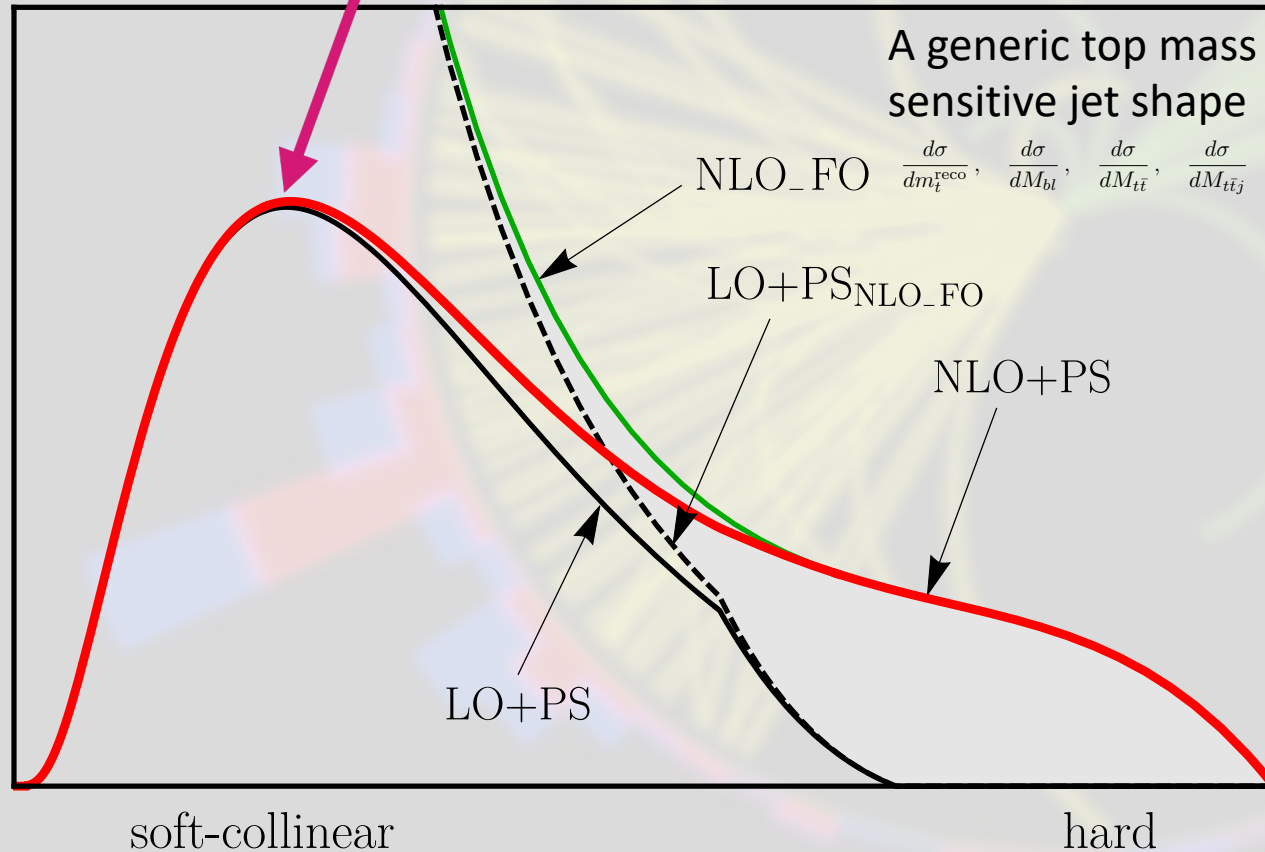
- Or can be computed from Monte Carlo Event generators...

- This is where best experimental precision has been achieved **We will come back to this in 2 slides**



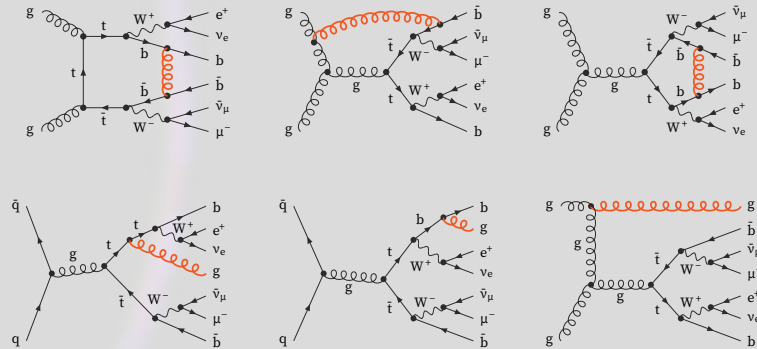
Why is measuring m_t hard theoretically?

Threshold structure sensitive to m_t



Top Production and decay at NLO, NNLO

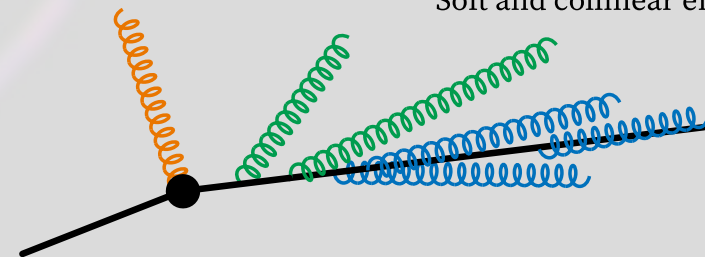
Mazzitelli et al. 2012.14267; Cormier et al. 1810.06493; Frederix et al. 1603.01178; Jezo et al. 1607.04538; Hoeche et al. 1402.6293



1207.5018

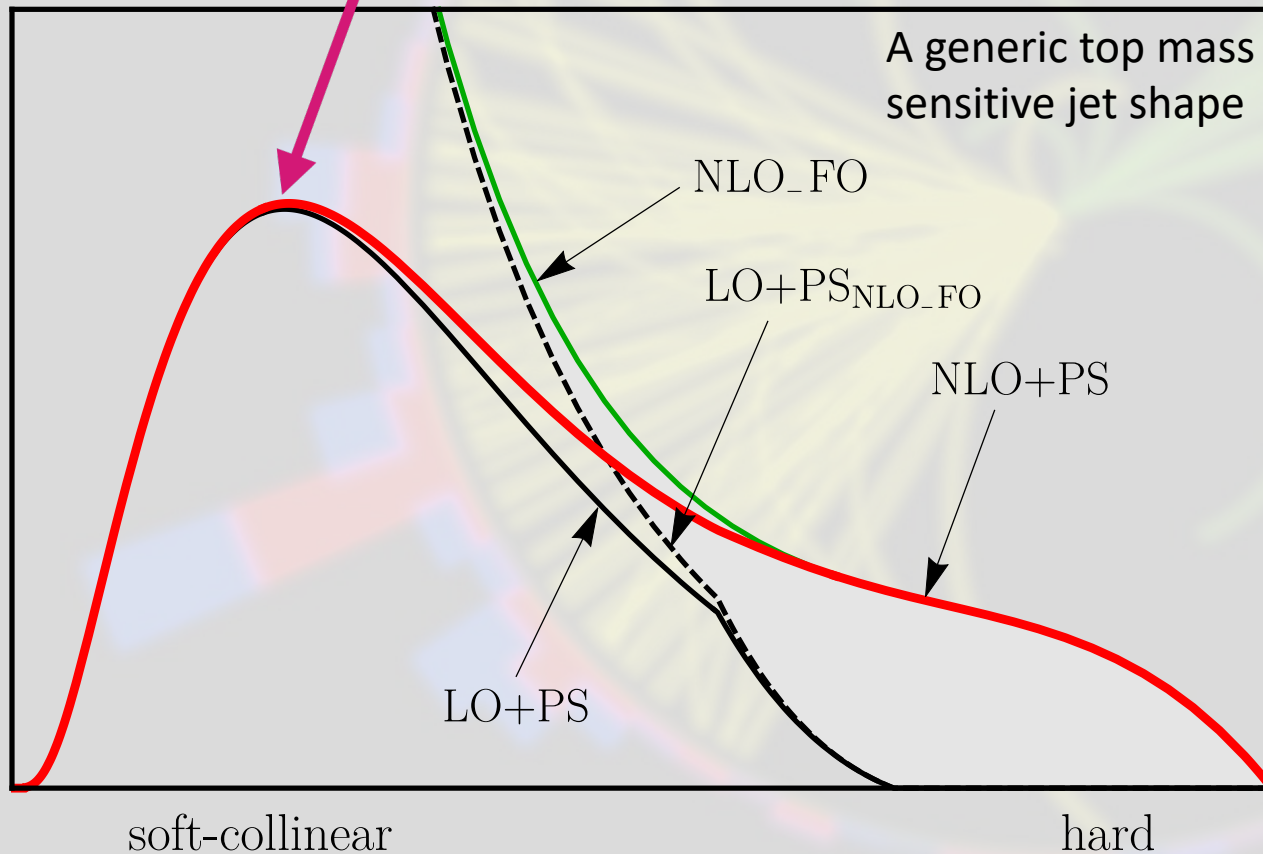
First hard emission

Soft and collinear emissions



Why is measuring m_t hard theoretically?

Threshold structure sensitive to m_t

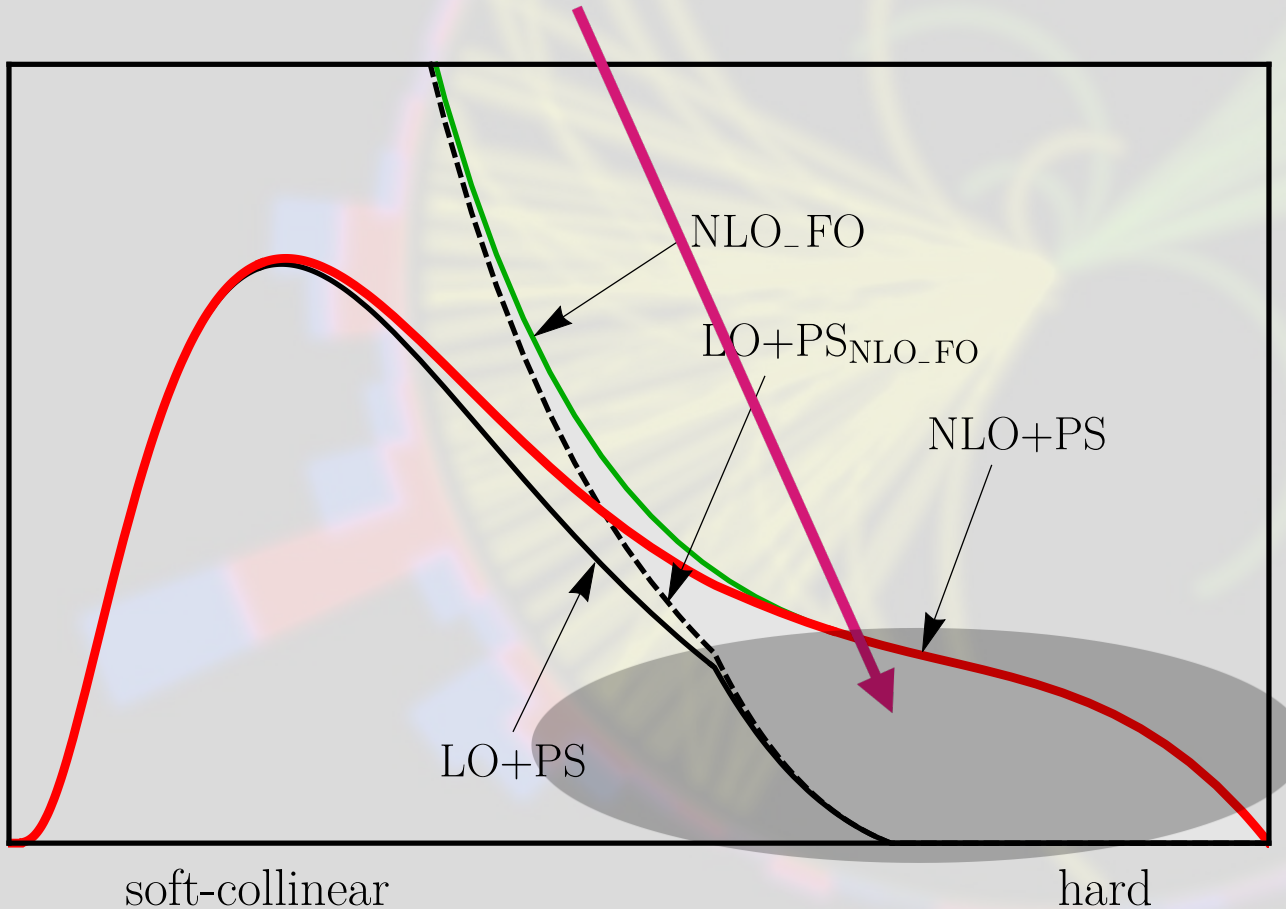


Observations:

- Threshold structure typically appears in the region where shape is dominated by **soft-collinear radiation**.
 - **Almost entirely dependent on parton shower or complicated resummation.**
- NLO corrections make an impact **only in the tail**.
 - High accuracy fixed order computations are only weakly m_t dependent.

Summary: measuring m_t is challenging

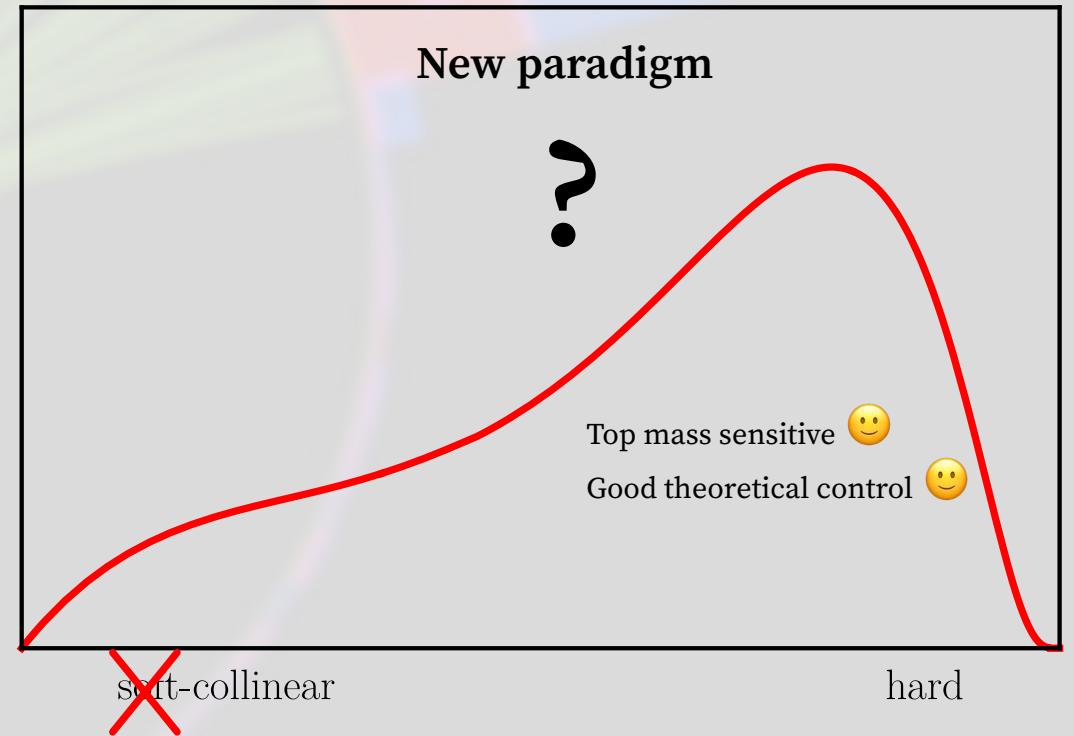
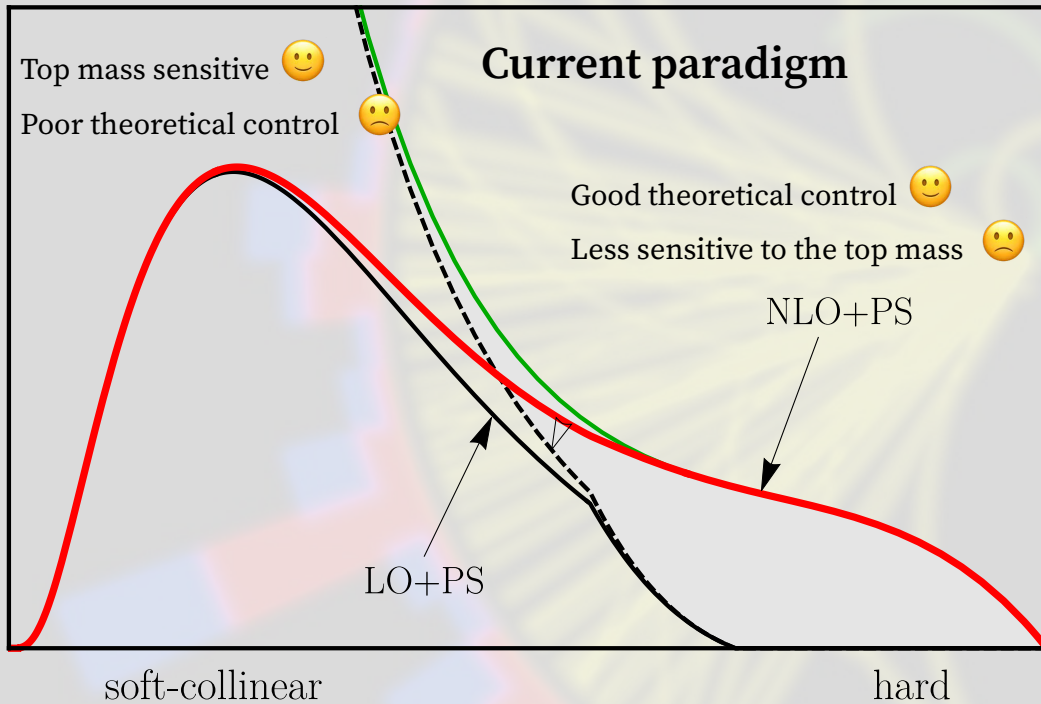
Focus here for good theoretical control, here PS is not dominant but a well controlled small perturbation.



ATLAS+CMS Preliminary LHC _{top} WG		m_{top} from cross-section measurements		Sep 2019
	total	stat	$m_{\text{top}} \pm \text{tot (stat} \pm \text{syst} \pm \text{theo)}$	Ref.
$\sigma(t\bar{t})$ inclusive, NNLO+NNLL				
ATLAS, 7+8 TeV			172.9 $^{+2.5}_{-2.6}$	[1]
CMS, 7+8 TeV			173.8 $^{+1.7}_{-1.8}$	[2]
CMS, 13 TeV			169.9 $^{+1.9}_{-2.1}$ (0.1 \pm 1.5 $^{+1.2}_{-1.5}$)	[3]
ATLAS, 13 TeV			173.1 $^{+2.0}_{-2.1}$	[4]
$\sigma(t\bar{t}+1j)$ differential, NLO				
ATLAS, 7 TeV			173.7 $^{+2.3}_{-2.1}$ (1.5 \pm 1.4 $^{+1.0}_{-0.5}$)	[5]
CMS, 8 TeV			169.9 $^{+4.5}_{-3.7}$ (1.1 $^{+2.5}_{-3.1}$ $^{+3.6}_{-1.6}$)	[6]
ATLAS, 8 TeV			171.1 $^{+1.2}_{-1.0}$ (0.4 \pm 0.9 $^{+0.7}_{-0.3}$)	[7]
$\sigma(t\bar{t})$ n-differential, NLO				
ATLAS, n=1, 8 TeV			173.2 \pm 1.6 (0.9 \pm 0.8 \pm 1.2)	[8]
CMS, n=3, 13 TeV			170.9 \pm 0.8	[9]
m_{top} from top quark decay				
	CMS, 7+8 TeV comb. [10]			
	ATLAS, 7+8 TeV comb. [11]			

Unfortunately, **poor sensitivity when not leveraging the threshold**

A new approach



[2004.12915](#) and S. Plätzer

A new approach

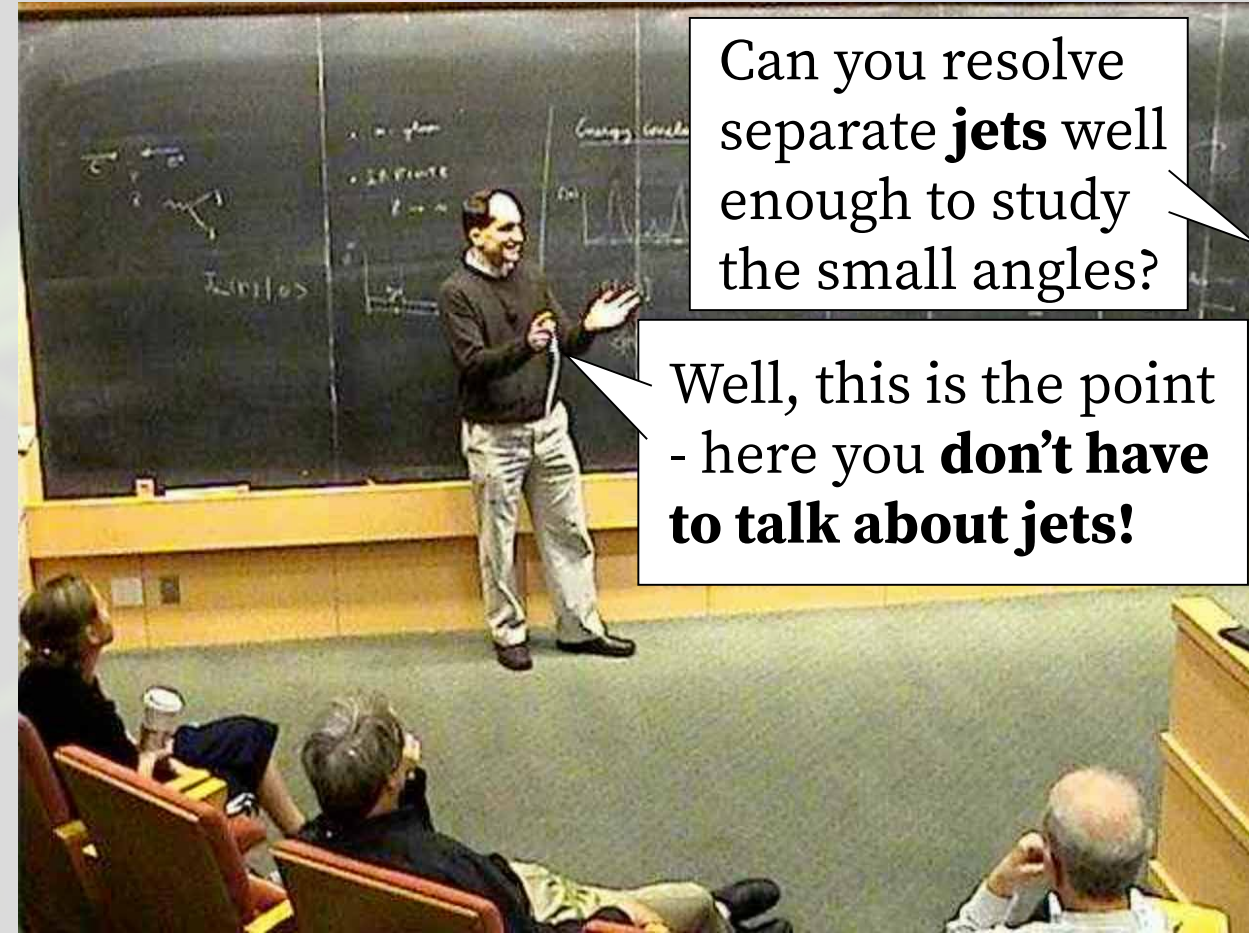
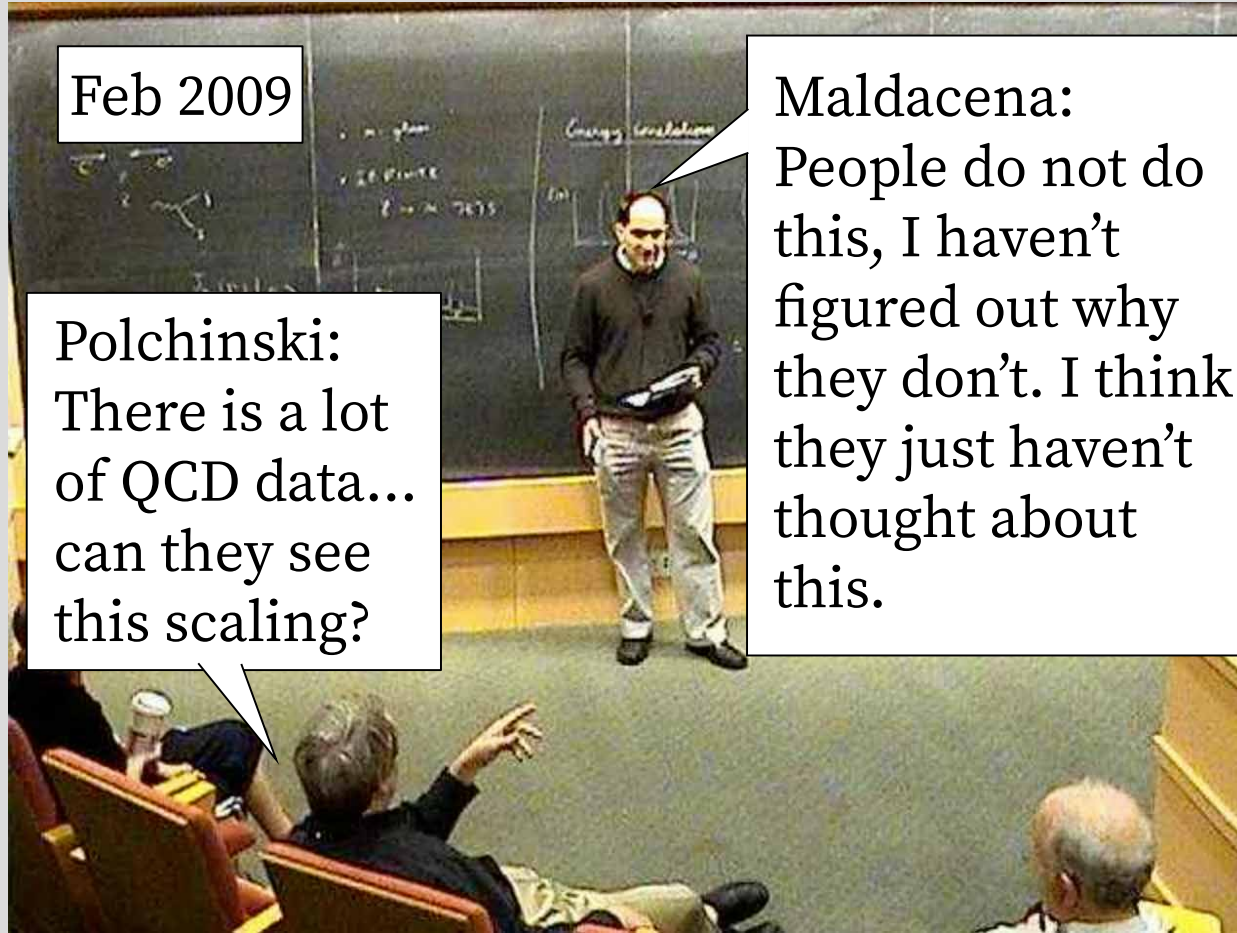
Let us re-think the problem somewhat. What do we have to work with?

- A (partial*) kinematic breakdown of the particles in each jet.
- A lot of statistics!
 - The HL-LHC will be a top factory.
 - It is forecast that 3Billion ttbar events and 800Million mono-top events will be measured. [1902.04070](#)

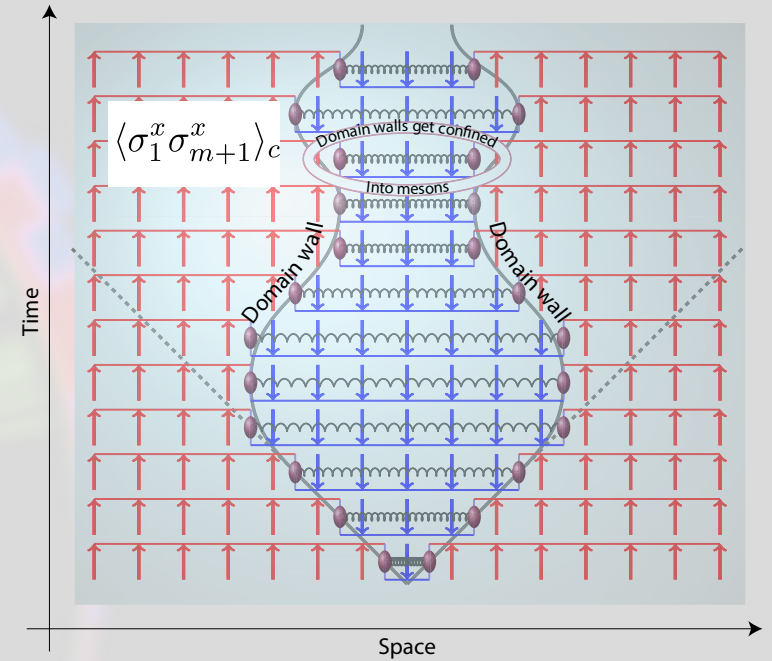
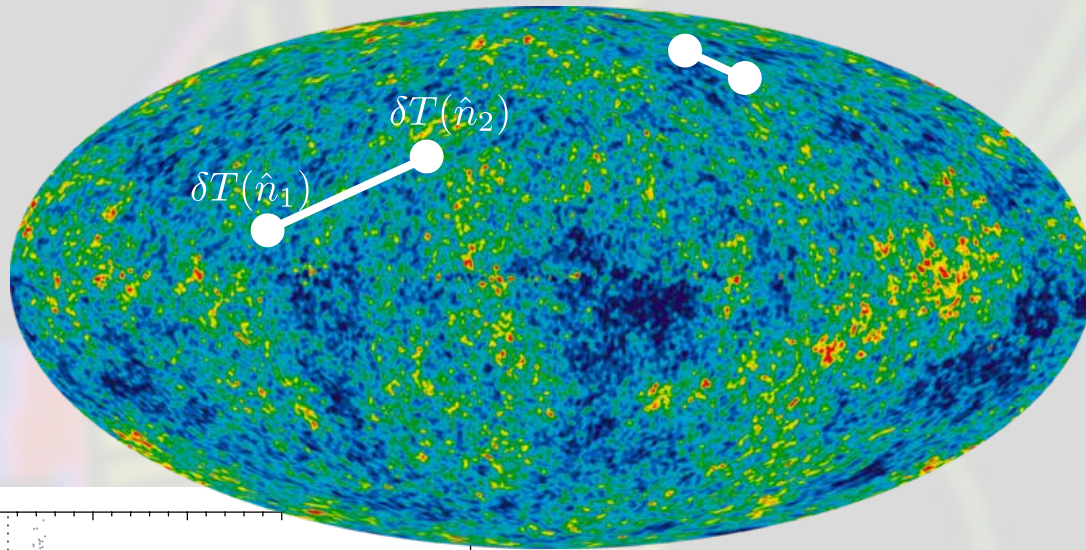
What observables do other fields of physics use when trying to extract simple properties from complicated environments with high statistics?

Correlation functions!

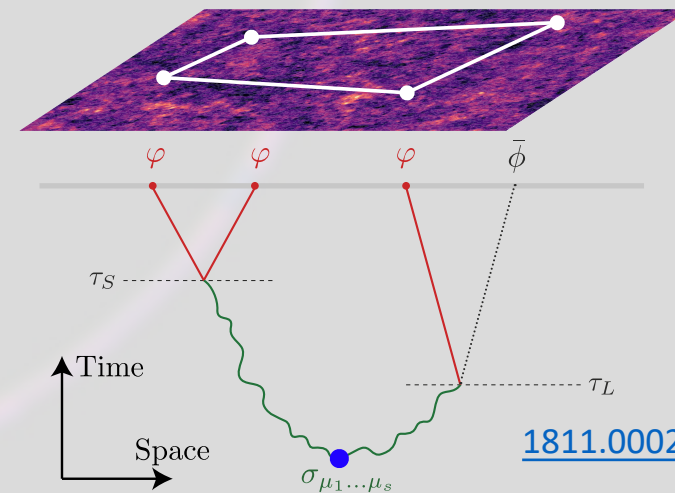
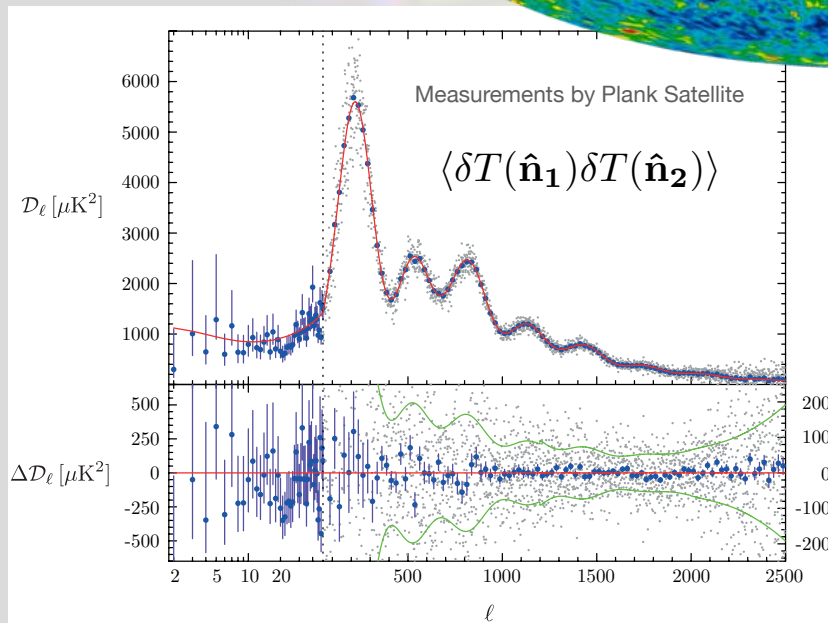
Part 2: Correlation functions



Correlation Functions



[1604.03571](#)



[1811.00024](#), [1503.08043](#)

Correlation Functions

Recap

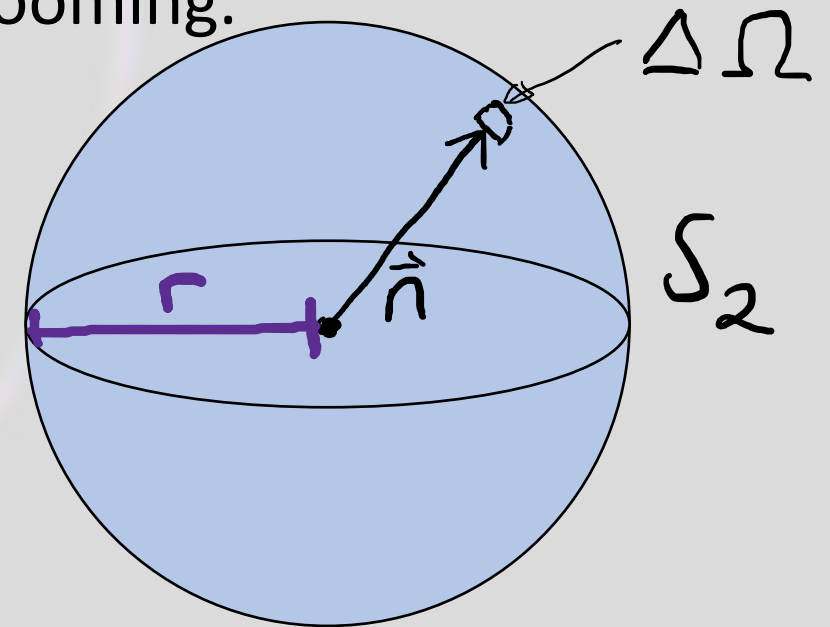
- Correlation functions in statistics:
 - $\text{Corr}_2(X, Y) = \langle XY \rangle - \langle X \rangle \langle Y \rangle$ (also just the covariance)
 - $\text{Corr}_3(X, Y, Z) = \langle XYZ \rangle - \langle X \rangle (\langle Y \rangle \langle Z \rangle - \text{Corr}_2(Y, Z))$
 - ...
- In physics we usually refer to $\langle X_1 \dots X_n \rangle$ as an n point correlator. This is just conventional and has origins in that often $\langle X_i \rangle = 0$.
- QFT correlators (propogators) relate back to these statistical correlators through the path integral and statistical mechanics...

Correlation Functions

- Generally one can define correlators of any quantum charge or conserved quantity.
- For QCD, correlators of energy flux are usually of most interest – these naturally remove soft physics without grooming.

$$\mathcal{E}(\vec{n}) = \lim_{r \rightarrow \infty} \int_0^{\infty} dt r^2 n^i T_{0i}(t, r\vec{n})$$

$$\mathcal{E}(\vec{n}) \approx \int_0^{\infty} dt E_{\text{flux through } \Delta\Omega}(t)$$

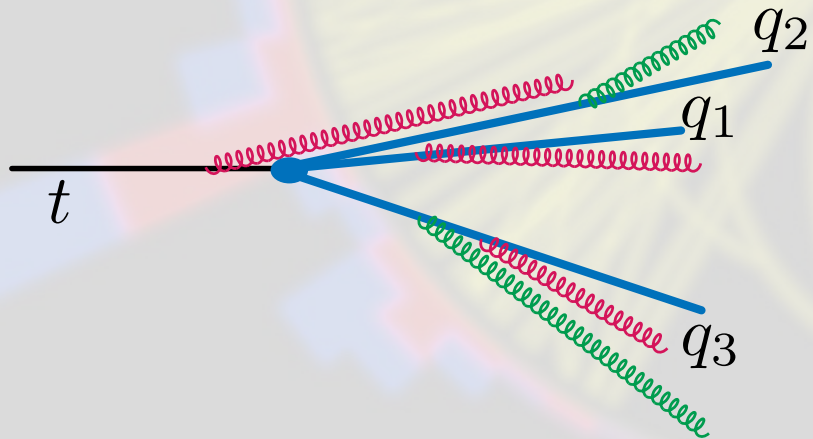


Correlation Functions

$$\mathcal{E}(\vec{n}) = \lim_{r \rightarrow \infty} \int_0^{\infty} dt r^2 n^i T_{0i}(t, r\vec{n})$$

$$\langle \mathcal{E}(\vec{n}_1) \mathcal{E}(\vec{n}_2) \rangle = \sum_{ij} \int \frac{d\sigma_{ij}}{d^2\vec{n}_i d^2\vec{n}_j} E_i E_j \delta^2(\vec{n}_1 - \vec{n}_i) \delta^2(\vec{n}_2 - \vec{n}_j)$$

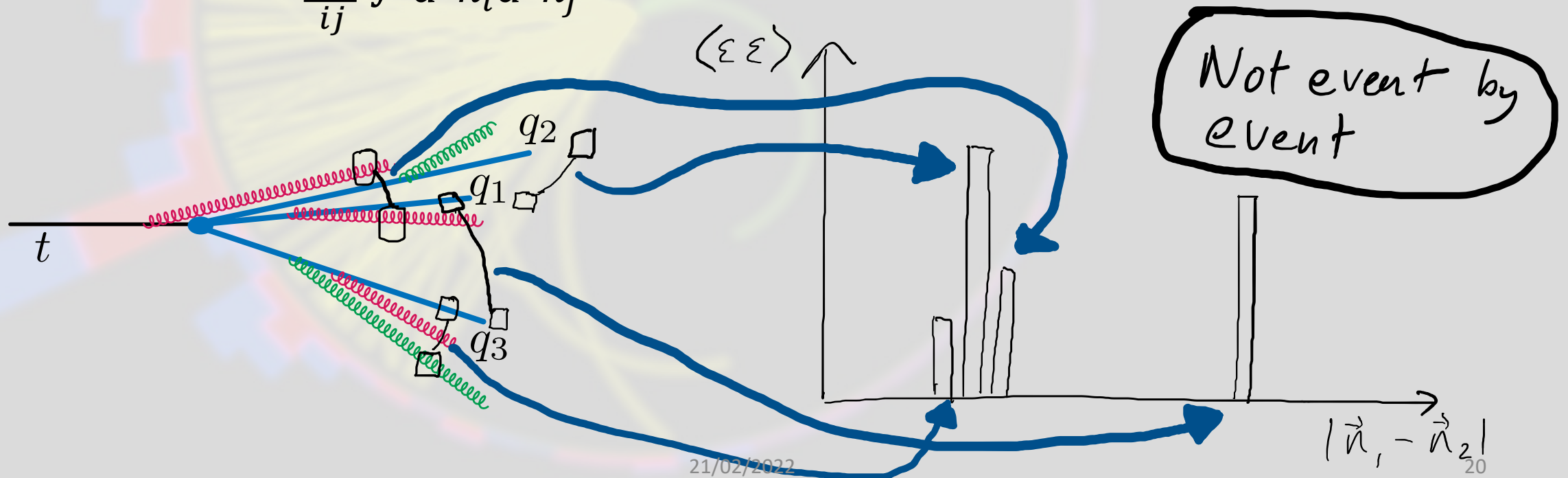
inclusive cross section to produce two particles, ij , and anything else!



Correlation Functions

$$\mathcal{E}(\vec{n}) = \lim_{r \rightarrow \infty} \int_0^{\infty} dt r^2 n^i T_{0i}(t, r\vec{n})$$

$$\langle \mathcal{E}(\vec{n}_1) \mathcal{E}(\vec{n}_2) \rangle = \sum_{ij} \int \frac{d\sigma_{ij}}{d^2\vec{n}_i d^2\vec{n}_j} E_i E_j \delta^2(\vec{n}_1 - \vec{n}_i) \delta^2(\vec{n}_2 - \vec{n}_j)$$



Correlation Functions

Pros:

- Defined on inclusive cross-sections and can be made insensitive to soft radiation. Textbook example of where pp CSS factorisation can be used without any violation. [2109.03665](#)

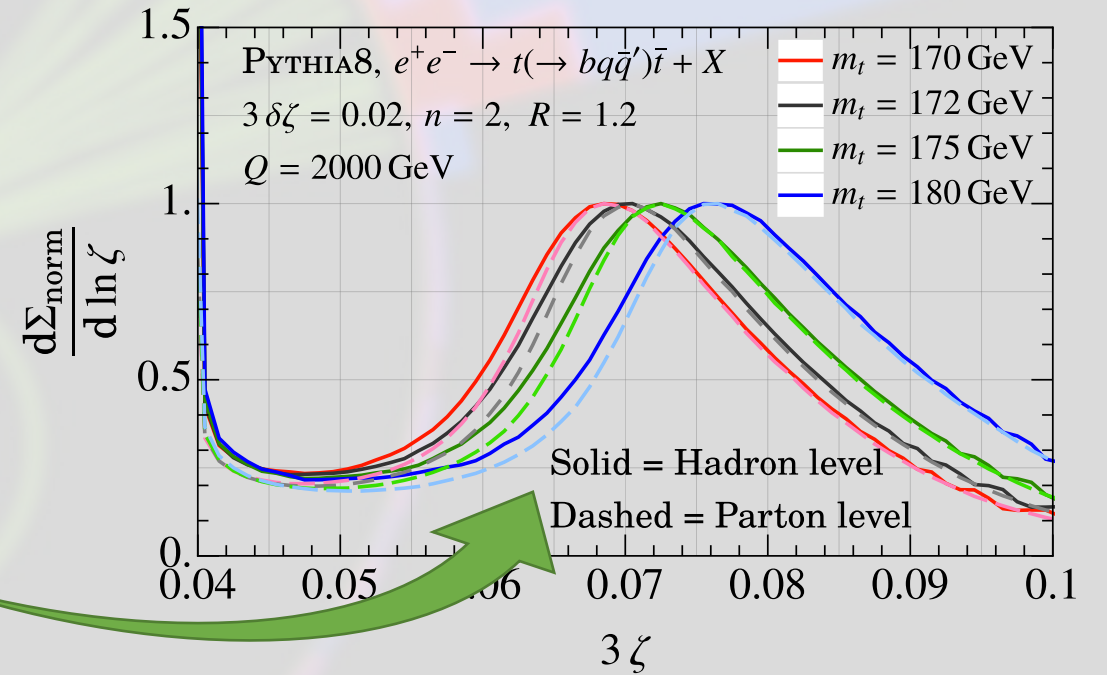
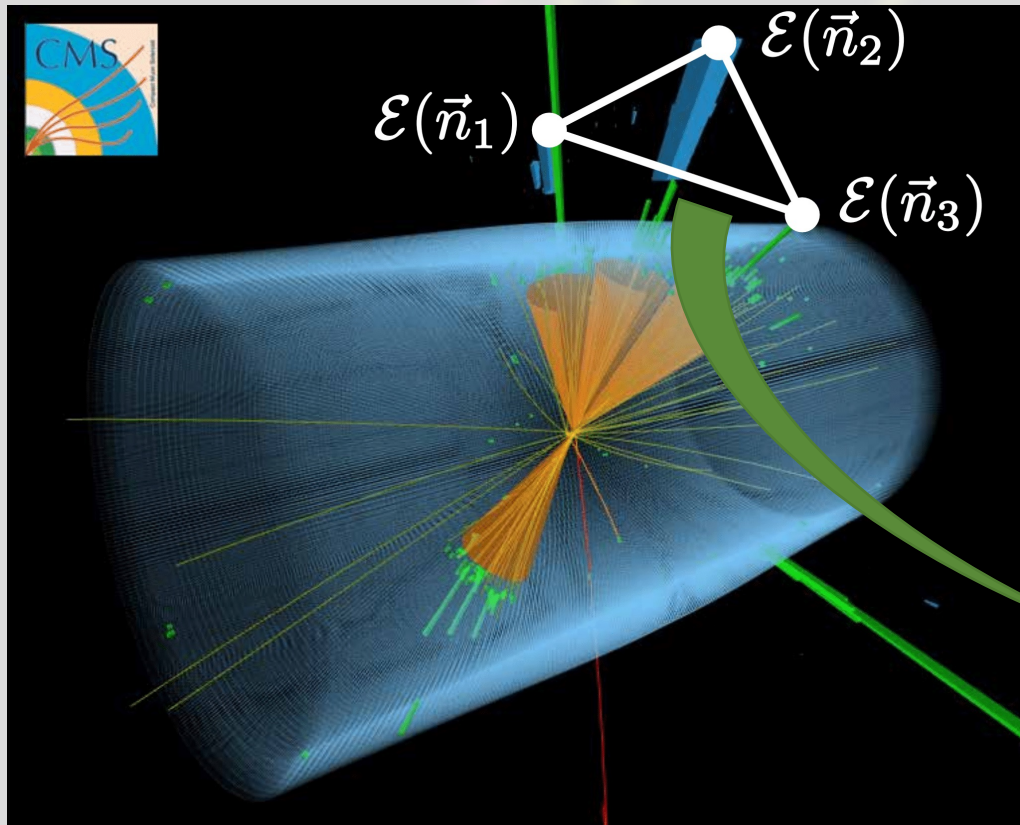
$$\frac{d\sigma}{d\zeta} = \int dE_J E_J^2 H(E_J) J_{\text{EEC}}(\zeta, E_J) + \text{power corrections},$$

- Well studied by CFT community. Powerful techniques exist for calculations: light-ray OPE, celestial Blocks, lorentzian inversion. [2202.04085](#)

Cons:

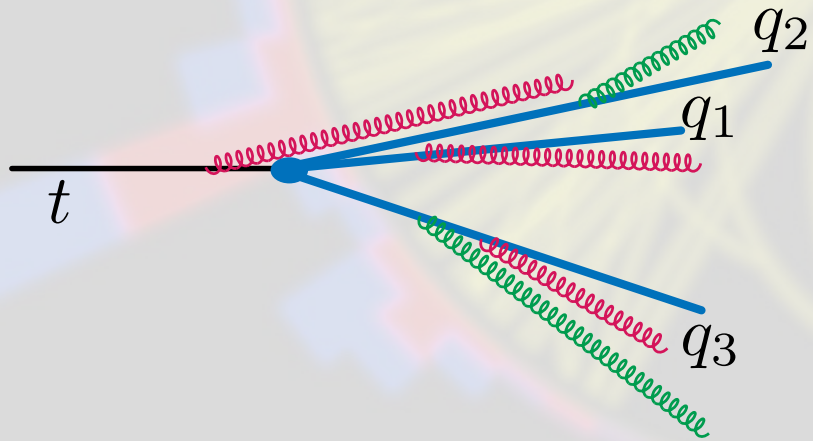
- Reliant on high stats. A precision tool, not a typical discovery tool.
- Not event-by-event so cannot be directly used to tag.

Part 3: Energy Correlators for Tops



Energy Correlators for Tops

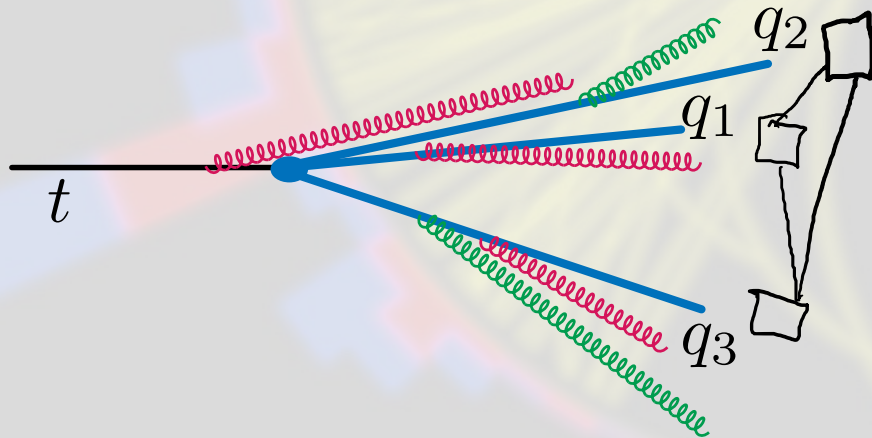
Which correlator will well characterise the top decay?



Energy Correlators for Tops

Which correlator will well characterise the top decay?

$$\langle \mathcal{E}(\vec{n}_1) \mathcal{E}(\vec{n}_2) \mathcal{E}(\vec{n}_3) \rangle = \sum_{ij} \int \frac{d\sigma_{ijk}}{d^2\vec{n}_i d^2\vec{n}_j d^2\vec{n}_k} E_i E_j E_k \delta^2(\vec{n}_1 - \vec{n}_i) \delta^2(\vec{n}_2 - \vec{n}_j) \delta^2(\vec{n}_2 - \vec{n}_k)$$



Energy Correlators for Tops

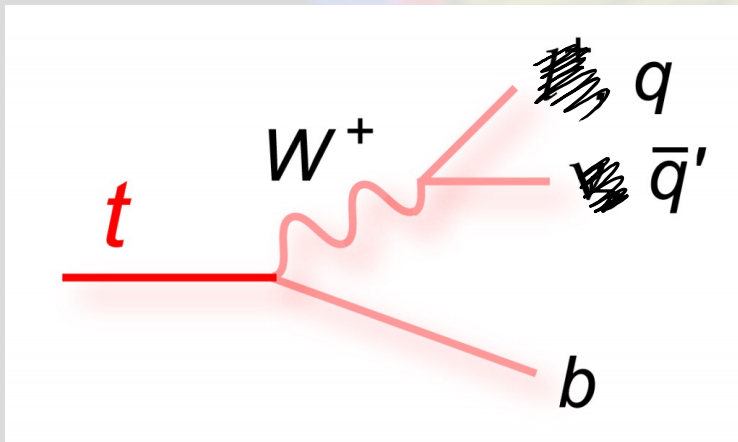
The correlator is sensitive to the angles between the decay products. What angles do we expect to see at fixed order?

I'm going to sketch a 'back of the envelope' calculation which gives intuition for the observable.

3-body kinematics

The correlator is sensitive to the angles between the decay products. What angles do we expect to see at fixed order?

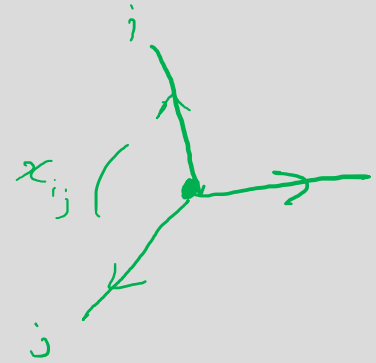
$$\{ ij = \frac{p_i \cdot p_j}{2} = \frac{(1 - \cos \theta_{ij})}{2} \approx \frac{\theta_{ij}^2}{4}$$



3-body kinematics

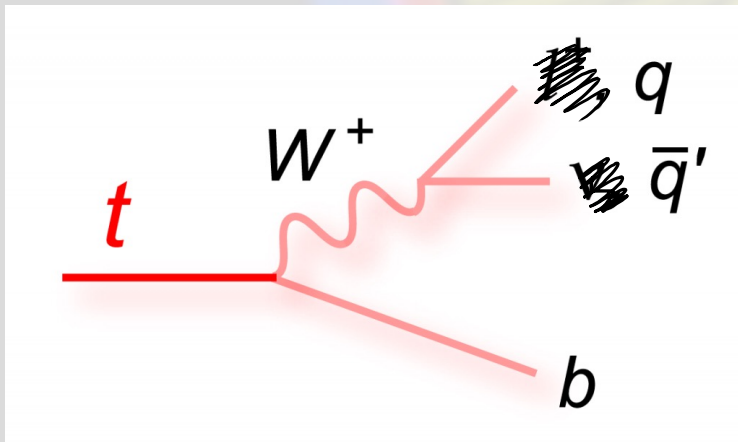
The correlator is sensitive to the angles between the decay products. What angles do we expect to see at fixed order?

$$\{ ij = \frac{p_i \cdot p_j}{2} = \frac{(1 - \cos \theta_{ij})}{2} \approx \frac{\theta_{ij}^2}{4}$$



In the Top rest frame

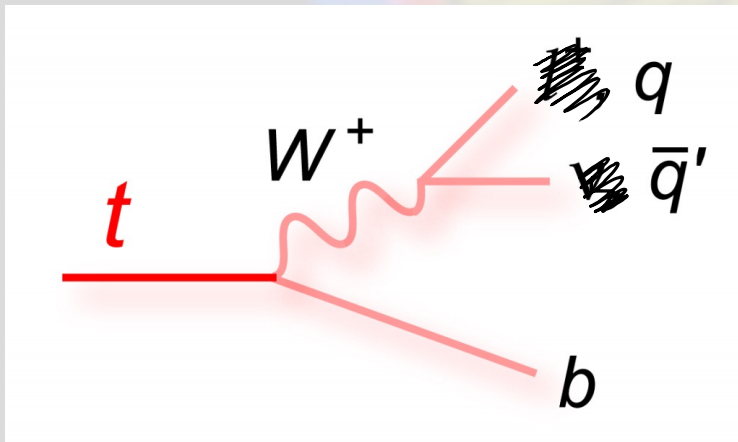
$$\{ 12 + \{ 23 + \{ 31 \in [2, 2.25]$$



3-body kinematics

The correlator is sensitive to the angles between the decay products. What angles do we expect to see at fixed order?

One can find the boost from the Top rest frame to the lab frame where we measure angles $\tilde{\zeta}_{ij}$. We find that



$$\sum_{ij} \tilde{\zeta}_{ij} \approx \left(\frac{m_t}{Q}\right)^2 \sum_{ij} \zeta_{ij}$$

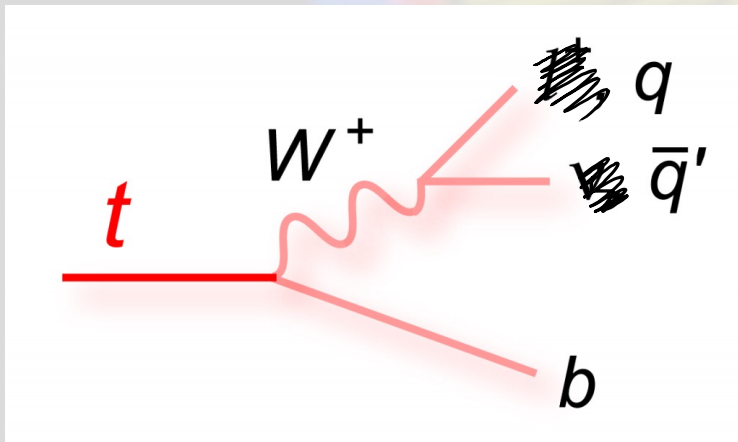
Building the observable

The correlator is sensitive to the angles between the decay products. What do we expect to see at fixed order?

Fixed order teaches us that look at

$$G(\{ \}) = \int d^2 \vec{n}_1 d^2 \vec{n}_2 d^2 \vec{n}_3 \langle \mathcal{E}(\vec{n}_1) \mathcal{E}(\vec{n}_2) \mathcal{E}(\vec{n}_3) \rangle$$

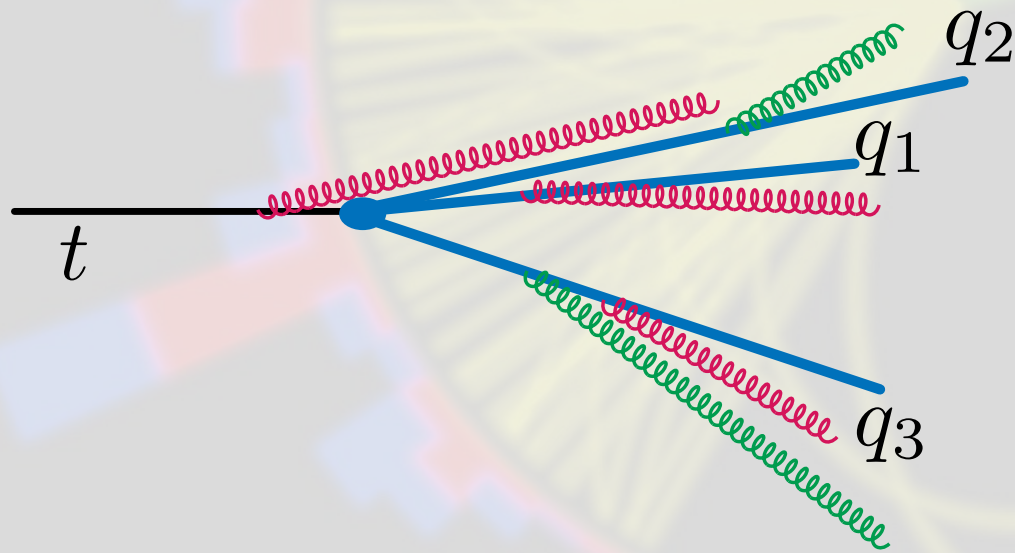
$$\times \delta(\{ \} - |\vec{n}_1 - \vec{n}_2| - |\vec{n}_2 - \vec{n}_3| - |\vec{n}_3 - \vec{n}_1|).$$



Doing the average over \vec{n}_i
 we find $\langle \{ \} \rangle \approx 3 \frac{m_c^2}{Q^2}$

Building the observable

What about higher order perturbative corrections?

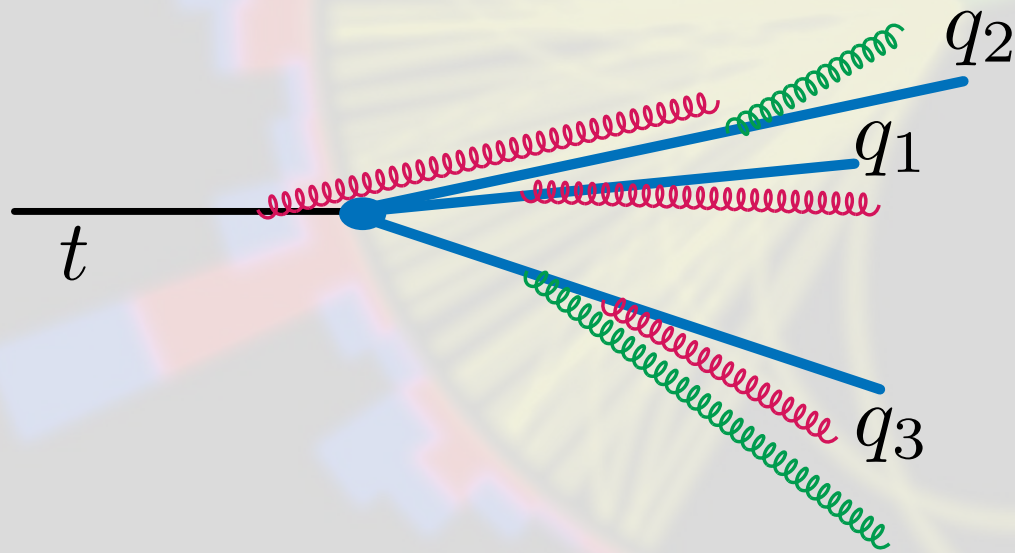


We want to preserve
the $\langle Z \rangle = 3 \frac{m_t^2}{Q^2}$ dependence!

Energy correlators not
sensitive to soft physics,
but will pick up collinear.
How to minimise?

Building the observable

What about higher order perturbative corrections?



Solution :

require $|\vec{n}_1 - \vec{n}_2| \approx |\vec{n}_2 - \vec{n}_3|$
 $\approx |\vec{n}_3 - \vec{n}_1|$

that way we never have
a small angle in the sum
over i, j around $\xi = \frac{3m_t^2}{Q^2}$.

Building the observable

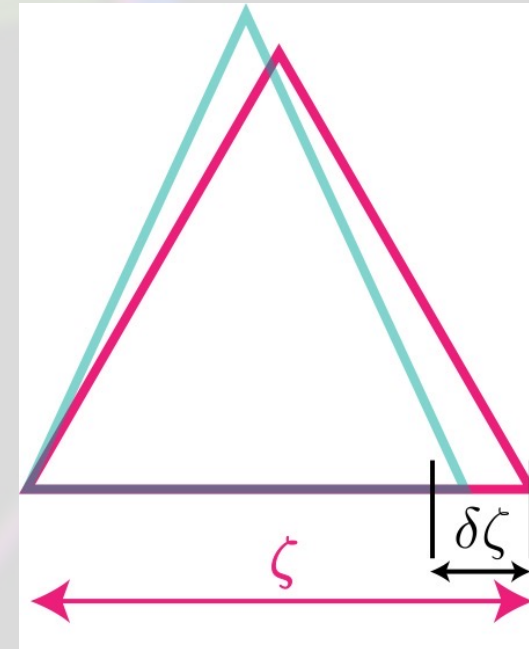
In all, we have...

$$\frac{d\Sigma(\delta\zeta)}{dQd\zeta} = \int d\zeta_{12}d\zeta_{23}d\zeta_{31} \int d\sigma \widehat{\mathcal{M}}_{\Delta}^{(n)}(\zeta_{12}, \zeta_{23}, \zeta_{31}, \zeta, \delta\zeta), \quad (4)$$

where the measurement operator $\widehat{\mathcal{M}}_{\Delta}^{(n)}$ is

$$\begin{aligned} \widehat{\mathcal{M}}_{\Delta}^{(n)}(\zeta_{12}, \zeta_{23}, \zeta_{31}, \zeta, \delta\zeta) &= \widehat{\mathcal{M}}^{(n)}(\zeta_{12}, \zeta_{23}, \zeta_{31}) \quad (5) \\ &\times \delta(3\zeta - \zeta_{12} - \zeta_{23} - \zeta_{31}) \prod_{l,m,n \in \{1,2,3\}} \Theta(\delta\zeta - |\zeta_{lm} - \zeta_{mn}|). \end{aligned}$$

$$\begin{aligned} \widehat{\mathcal{M}}^{(n)}(\zeta_{12}, \zeta_{23}, \zeta_{31}) &= \quad (2) \\ &\sum_{i,j,k} \frac{E_i^n E_j^n E_k^n}{Q^{3n}} \delta(\zeta_{12} - \hat{\zeta}_{ij}) \delta(\zeta_{23} - \hat{\zeta}_{ik}) \delta(\zeta_{31} - \hat{\zeta}_{jk}). \end{aligned}$$

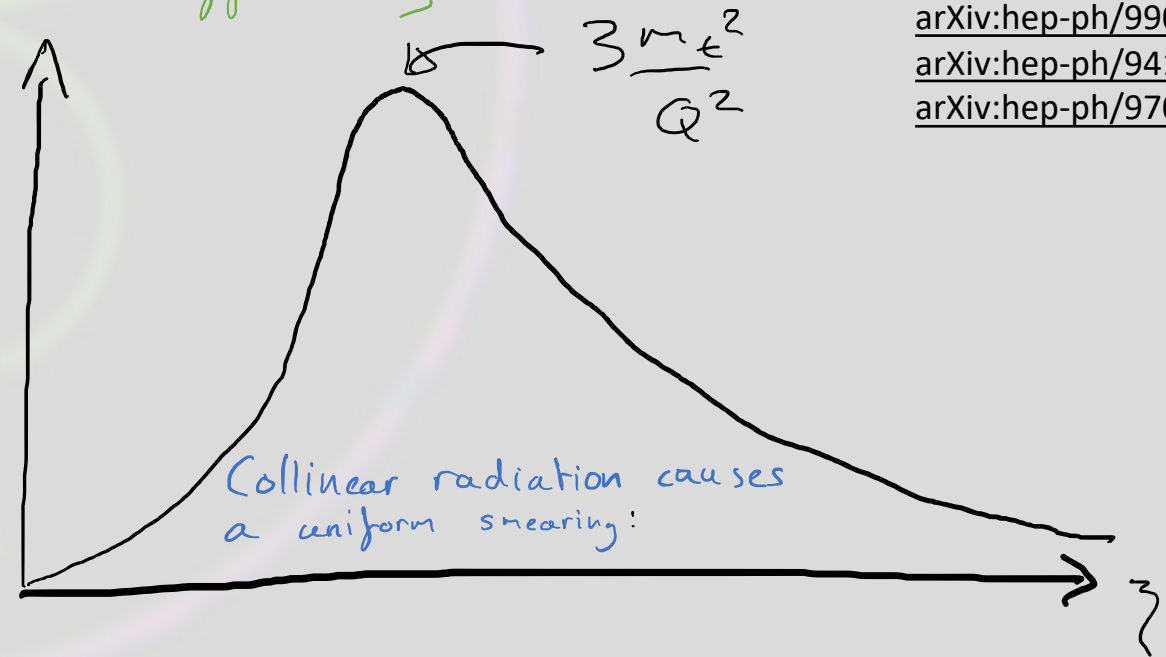
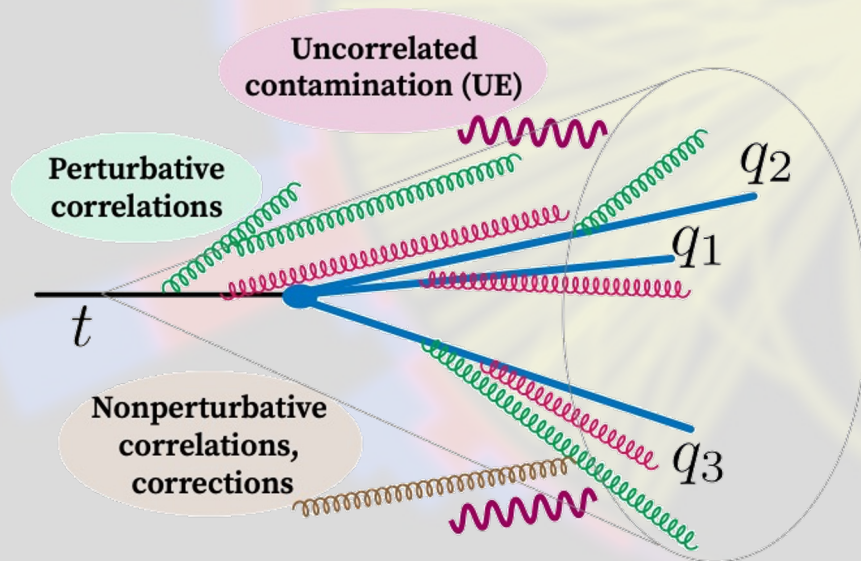


Understanding the distribution

What will the distribution look like with N.P. corrections?

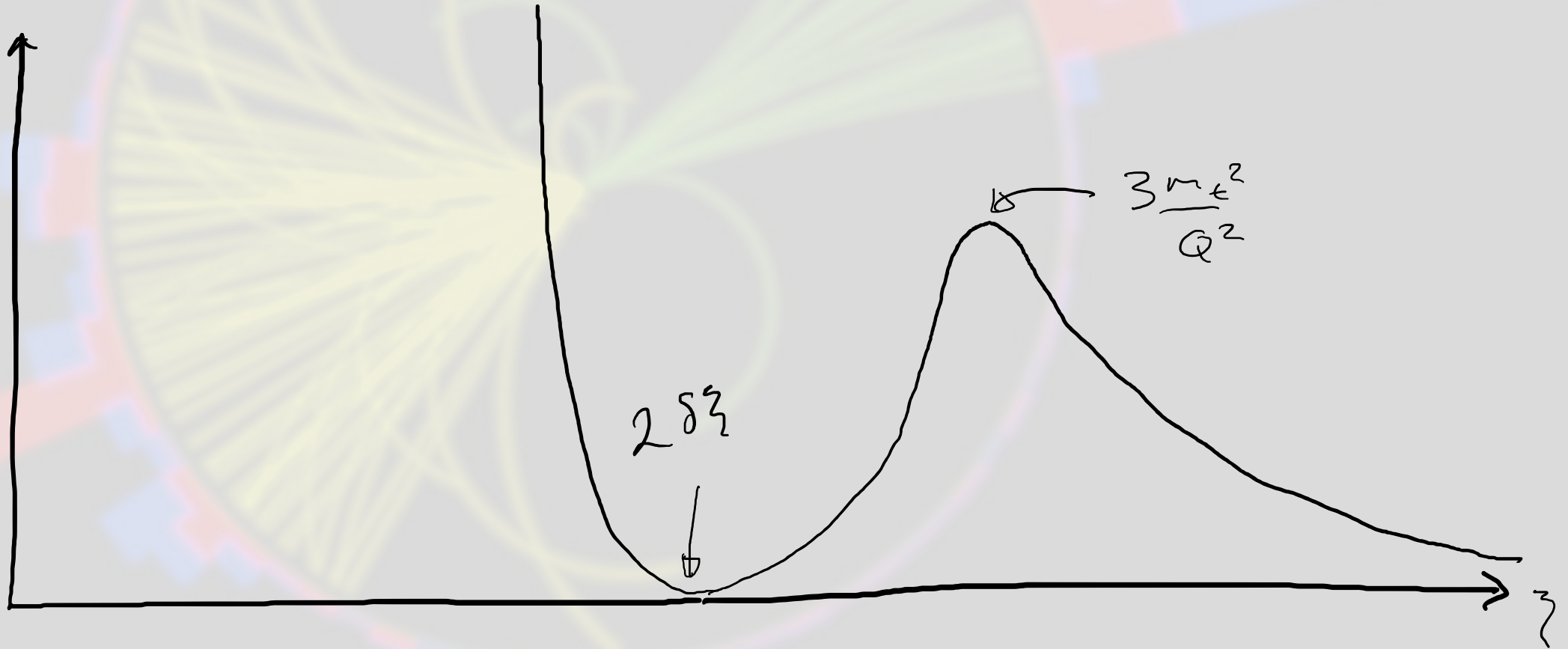
We know from other studies of energy correlators that N.P. corrections are an additive power law. Effectively a change in normalisation.

[arXiv:hep-ph/9902341](https://arxiv.org/abs/hep-ph/9902341)
[arXiv:hep-ph/9411211](https://arxiv.org/abs/hep-ph/9411211)
[arXiv:hep-ph/9708346](https://arxiv.org/abs/hep-ph/9708346)



Understanding the distribution

What is the effect of the asymmetry in the triangle?



Understanding the distribution

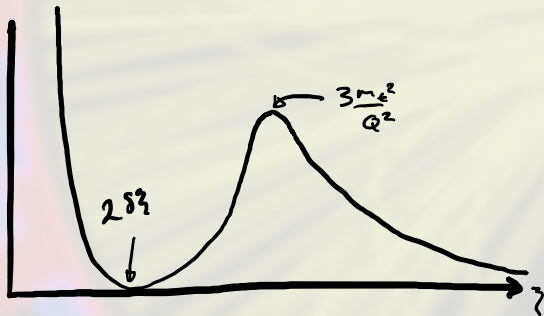
Enough sketching!

Let us simulate.

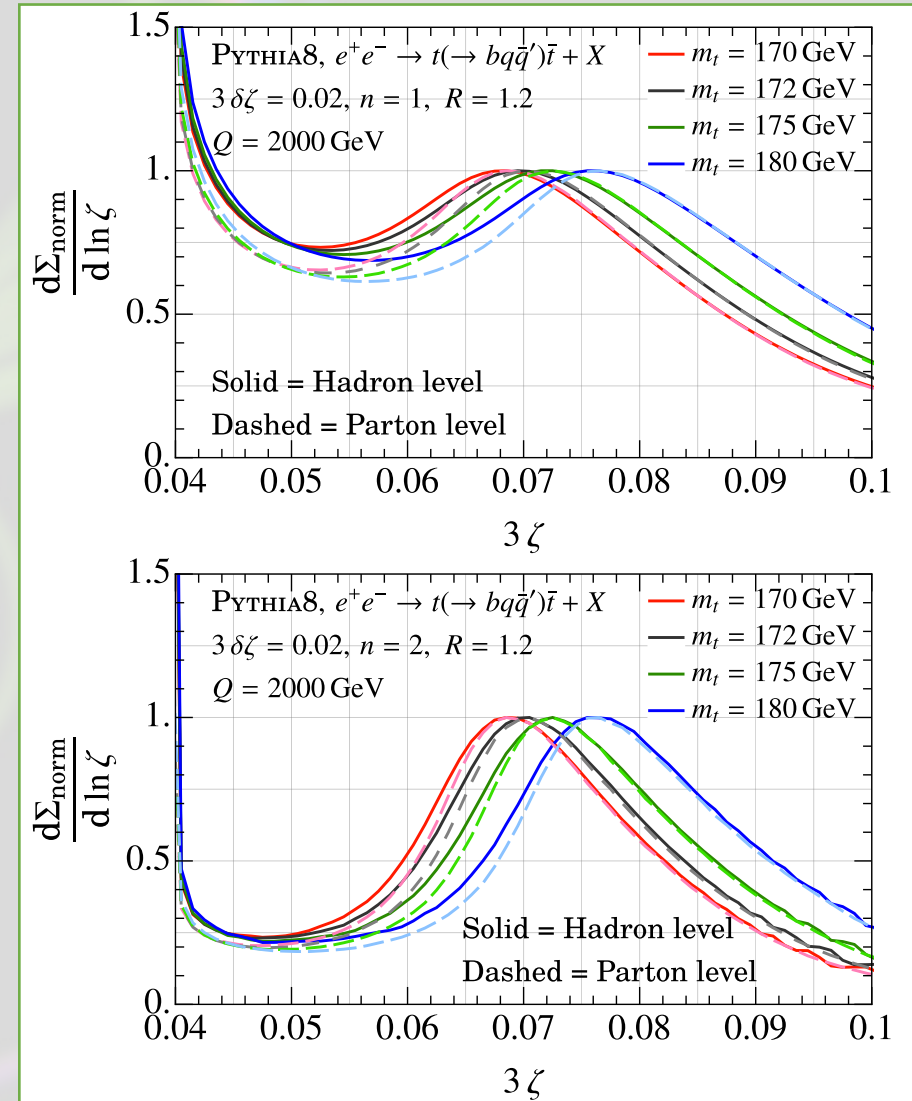
Simulation in Pythia8

We did a complete simulated pp analysis, however for this talk consider e^+e^- where the hard scale Q is just half the CoM Energy.

- Key features exactly as expected.



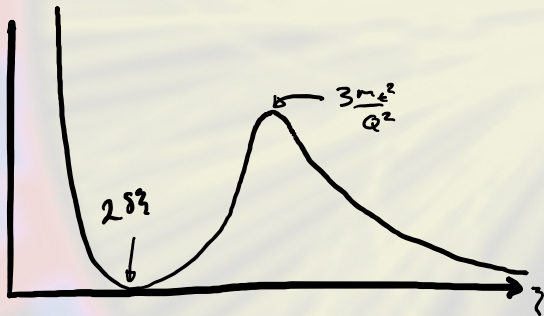
- Peak is sensitive to Top mass.
- Very low sensitivity to hadronisation. The shift is equivalent to $\Delta m_t = 150 \pm 50 \text{ MeV}$.



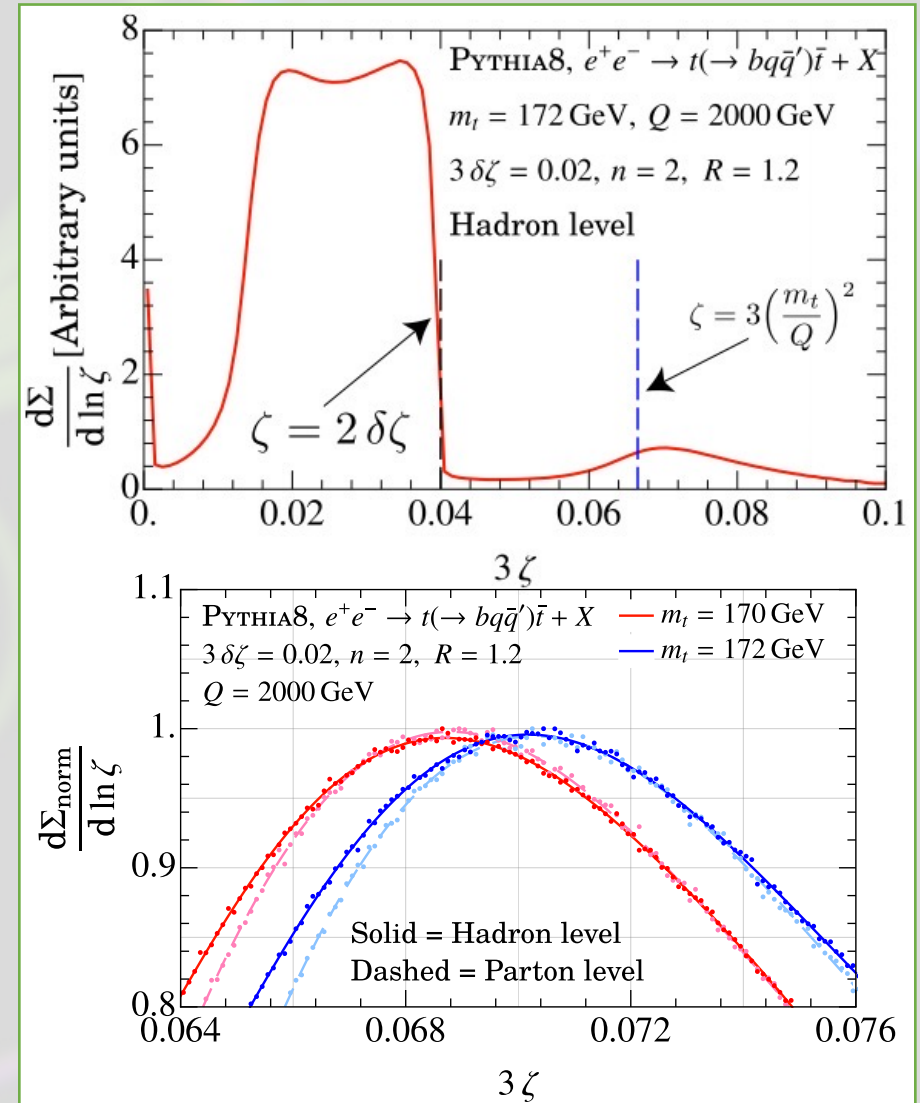
Simulation in Pythia8

We did a complete simulated pp analysis, however for this talk consider e^+e^- where the hard scale Q is just half the CoM Energy.

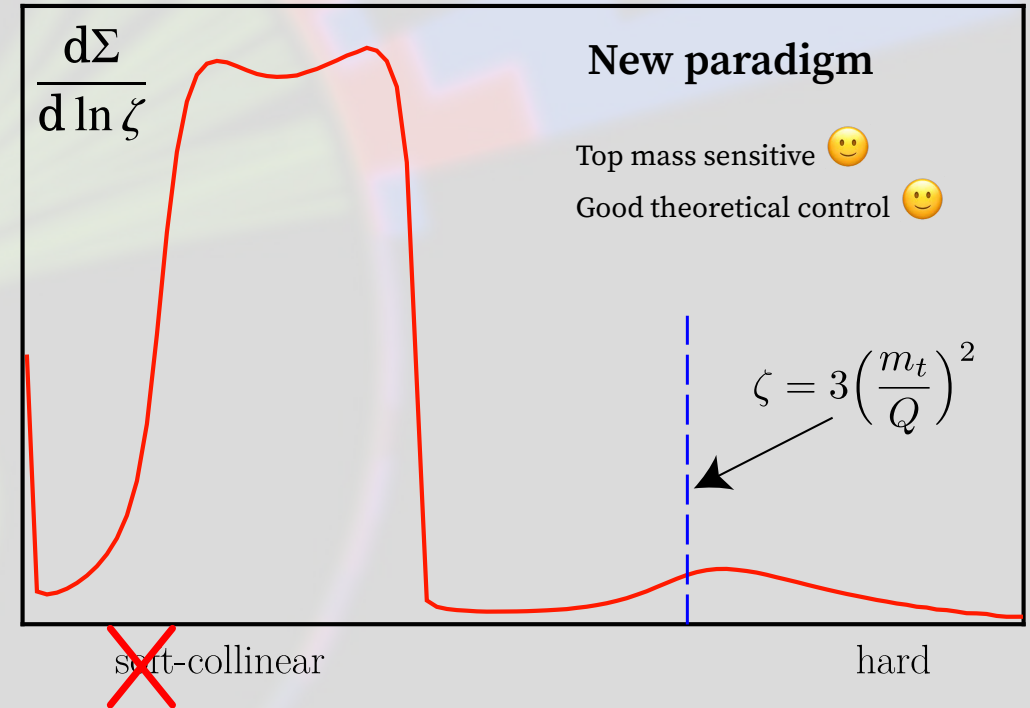
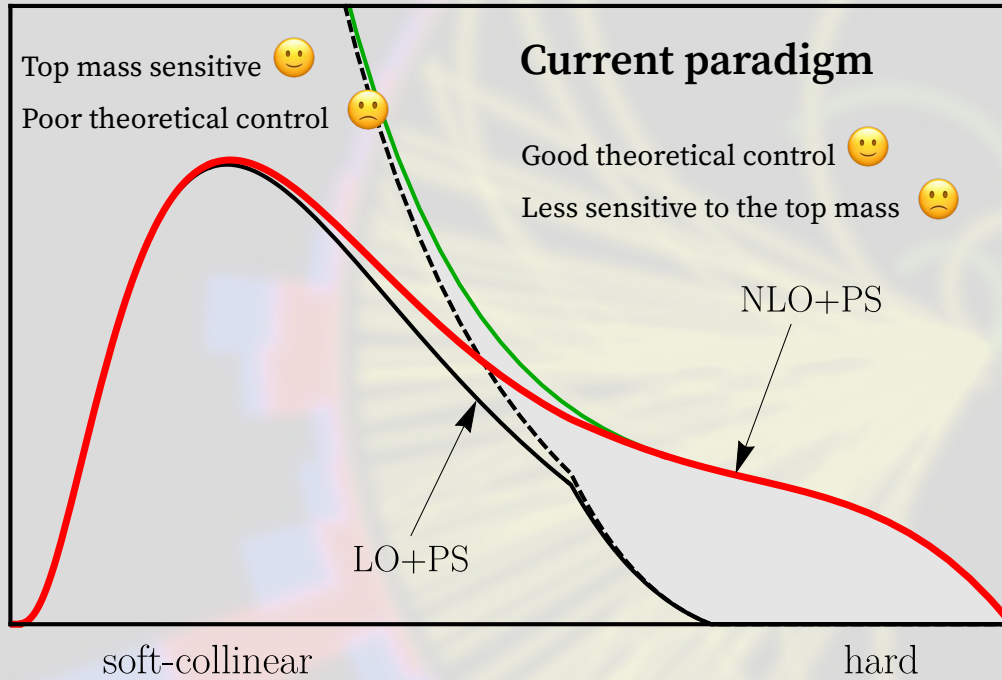
- Key features exactly as expected.



- Peak is sensitive to Top mass.
- Very low sensitivity to hadronisation. The shift is equivalent to $\Delta m_t = 150 \pm 50 \text{ MeV}$.



Conclusions



$$\frac{d\Sigma}{dp_{T,\text{jet}} d\eta d\zeta} = f_i \otimes f_j \otimes H_{i,j \rightarrow t} \left(z_J; p_{T,t} = \frac{p_{T,\text{jet}}}{z_J}, \eta \right)$$

$$\otimes J_{t \rightarrow t}(z_J, z_h; R) \otimes J_{\text{EEEC}}^{\text{[tracks]}}(n, z_h, \zeta; m_t; \Gamma_t)$$

Outlook

- The three-point energy correlator shows promise as a top mass sensitive observable with theoretical control comparable to the current precision of direct measurements.
- So far studies have been proof-of-concept. An experimental feasibility study would be prescient.
- Much of the ingredients needed for a precision calculation already exist. Missing pieces are the EEE jet function and a broader study of factorisation.

Simulation in Pythia8

Now consider hadron colliders. Must now use boost invariant quantities.

- Q is now the partonic Top p_T . This is not a measurable quantity. Instead we have the p_T of the Top jet. This adds a little complexity.

$$\frac{d\Sigma(\delta\zeta)}{dp_{T,\text{jet}}d\zeta} = \frac{d\Sigma(\delta\zeta)}{dp_{T,t}d\zeta} \frac{dp_{T,t}}{dp_{T,\text{jet}}}$$

- Now must consider underlying event.
- Can we measure on tracks? (Yes)

$$\widehat{\mathcal{M}}^{(n)}(\zeta_{12}, \zeta_{23}, \zeta_{31}) = \sum_{i,j,k} \frac{E_i^n E_j^n E_k^n}{Q^{3n}} \delta(\zeta_{12} - \hat{\zeta}_{ij}) \delta(\zeta_{23} - \hat{\zeta}_{ik}) \delta(\zeta_{31} - \hat{\zeta}_{jk}). \quad (2)$$



$$\widehat{\mathcal{M}}_{(pp)}^{(n)}(\zeta_{12}, \zeta_{23}, \zeta_{31}) = \sum_{i,j,k \in \text{jet}} \frac{(p_{T,i})^n (p_{T,j})^n (p_{T,k})^n}{(p_{T,\text{jet}})^{3n}} \times \delta(\zeta_{12} - \hat{\zeta}_{ij}^{(pp)}) \delta(\zeta_{23} - \hat{\zeta}_{ik}^{(pp)}) \delta(\zeta_{31} - \hat{\zeta}_{jk}^{(pp)}), \quad (7)$$

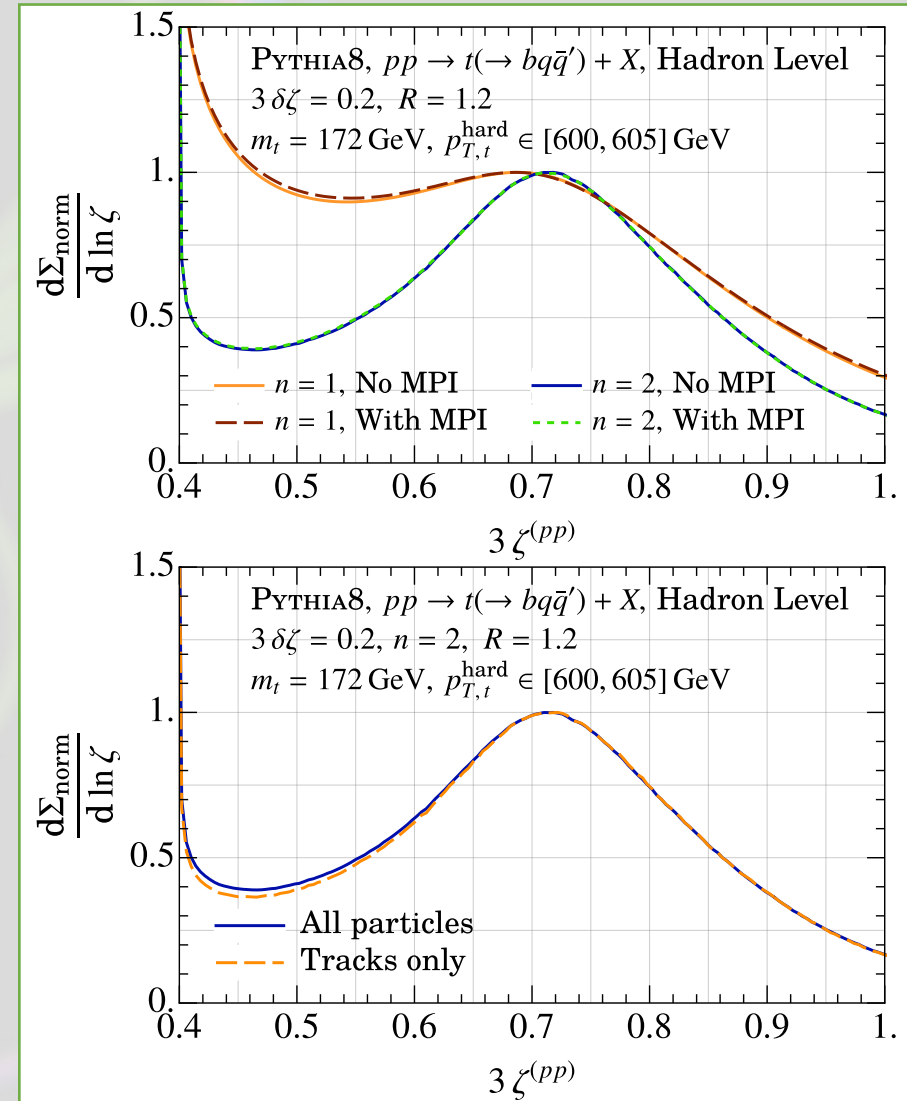
where $\hat{\zeta}_{ij}^{(pp)} = \Delta R_{ij}^2 = \sqrt{\Delta\eta_{ij}^2 + \Delta\phi_{ij}^2}$, with η, ϕ the standard rapidity, azimuth coordinates.

Simulation in Pythia8

Let us study the hadron collider environment in two parts.

1. First study the observable whilst unphysically fixing the partonic Top p_T . This is to answer:
 - Now must consider underlying event.
 - Can we measure on tracks? (Yes)
2. Then study the physical observable and in conjunction with the p_T spectrum.

Stage 1

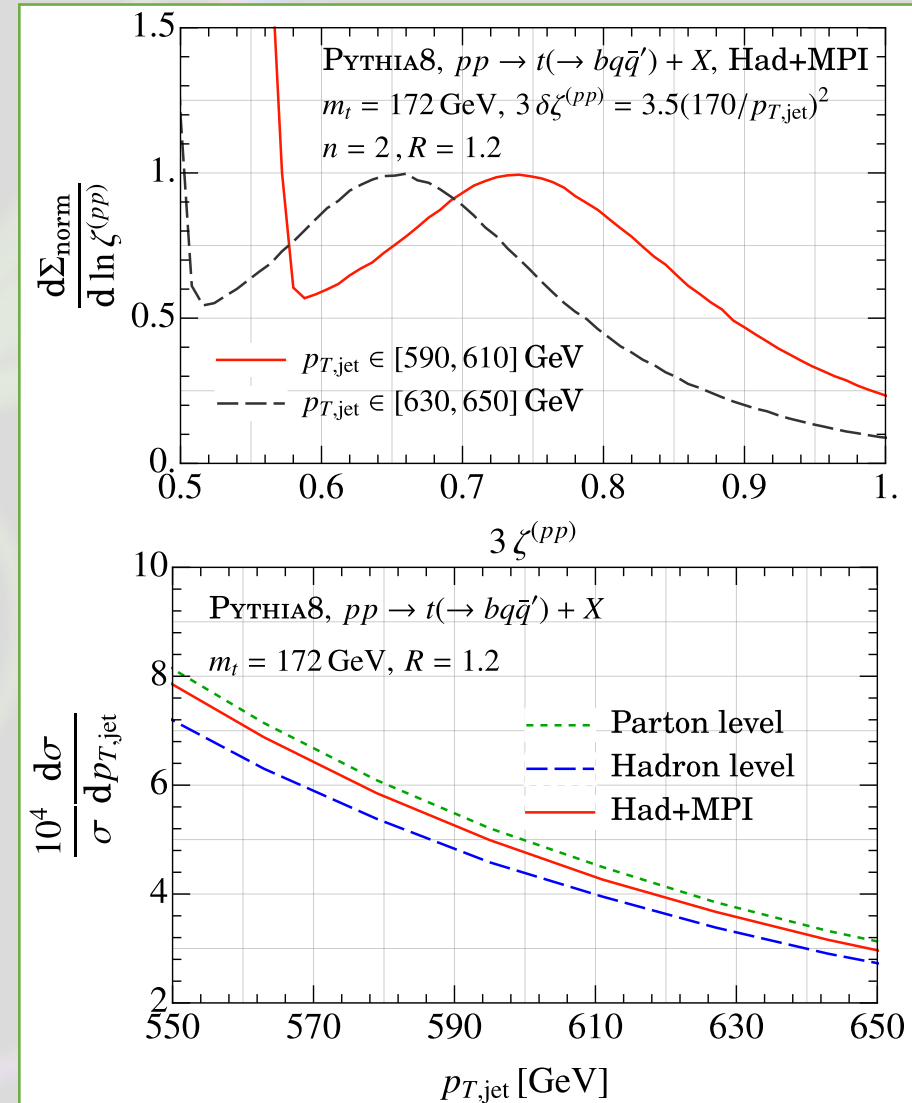


Simulation in Pythia8

Let us study the hadron collider environment in two parts.

1. First study the observable whilst unphysically fixing the partonic Top p_T . This is to answer:
 - Now must consider underlying event.
 - Can we measure on tracks? (Yes)
2. Then study the physical observable and in conjunction with the p_T spectrum.

Stage 2



Simulation in Pythia8

How to handle these p_T shifts? One method:

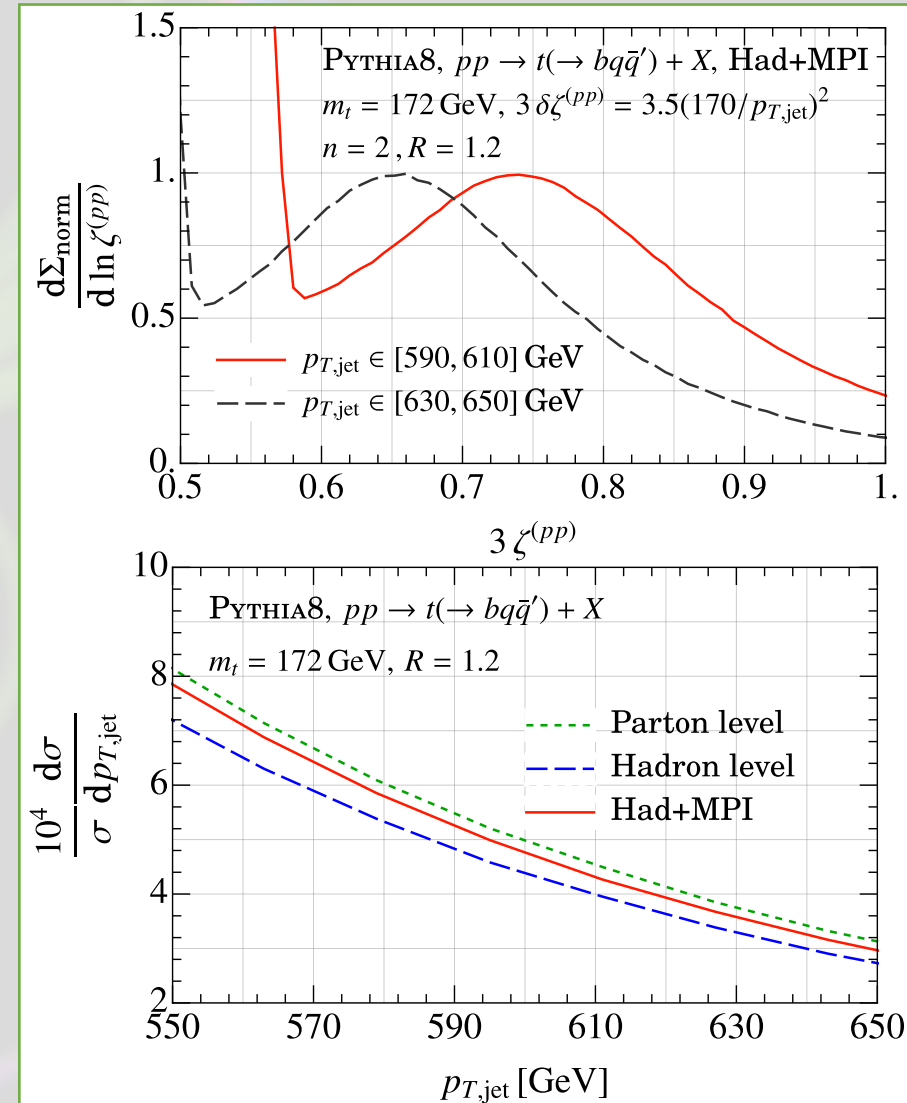
- Fixed order gives

$$\zeta_{\text{peak}}^{(pp)} \approx 3m_t^2 / p_{T,t}^2$$

- From Factorisation properties of the observable,

$$\zeta_{\text{peak}}^{(pp)} = \frac{3F_{\text{pert}}(m_t, p_{T,\text{jet}}, \alpha_s, R)}{(p_{T,\text{jet}} + \Delta_{\text{NP}}(R) + \Delta_{\text{MPI}}(R))^2}.$$

Stage 2



Simulation in Pythia8

How to handle these p_T shifts? One method:

- Fixed order gives

$$\zeta_{\text{peak}}^{(pp)} \approx 3m_t^2 / p_{T,t}^2$$

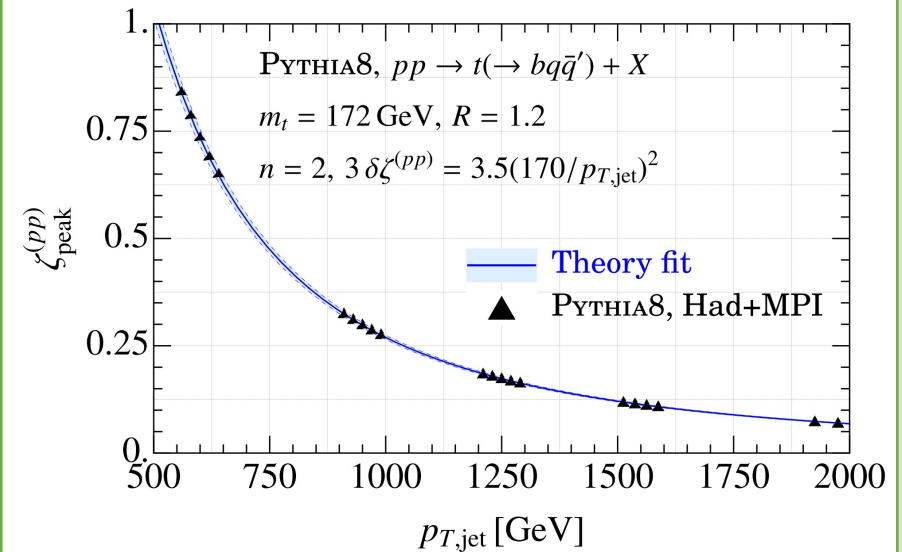
- From Factorisation properties of the observable,

$$\zeta_{\text{peak}}^{(pp)} = \frac{3F_{\text{pert}}(m_t, p_{T,\text{jet}}, \alpha_s, R)}{(p_{T,\text{jet}} + \Delta_{\text{NP}}(R) + \Delta_{\text{MPI}}(R))^2}.$$

Stage 2

PYTHIA8 m_t	Parton $\sqrt{F_{\text{pert}}}$	Hadron + MPI $\sqrt{F_{\text{pert}}}$
172 GeV	172.6 ± 0.3 GeV	$172.3 \pm 0.2 \pm 0.4$ GeV
173 GeV	173.5 ± 0.3 GeV	$173.6 \pm 0.2 \pm 0.4$ GeV
175 GeV	175.5 ± 0.4 GeV	$175.1 \pm 0.3 \pm 0.4$ GeV
173 – 172	0.9 ± 0.4 GeV	1.3 ± 0.6 GeV
175 – 172	2.9 ± 0.5 GeV	2.8 ± 0.6 GeV

TABLE I: Values of the effective parameter $F_{\text{pert}}(m_t)$ extracted at parton level, and hadron+MPI level. The consistency of the two approaches provides a measure of our uncertainty due to non-perturbative corrections.



Supplementary material

1. Parameterize the all orders peak position:

$$\zeta_{\text{peak}}^{(pp)} = 3(1 + \mathcal{O}(\alpha_s)) \frac{m_t^2}{f(p_{T,\text{jet}}, m_t, \alpha_s, \Lambda_{\text{QCD}})^2} \equiv 3(1 + \mathcal{O}(\alpha_s)) \frac{m_t^2}{(p_{T,\text{jet}} + \Delta(p_{T,\text{jet}}, m_t, \alpha_s, \Lambda_{\text{QCD}}))^2}$$

2. Work with

$$\rho^2(\zeta_{\text{peak}}^{(pp)v}, p_{T,\text{jet}}^v) = \left(\zeta_{\text{peak}}^{(pp)\text{ref}} - \zeta_{\text{peak}}^{(pp)v} \right) \left(\frac{3(1 + \mathcal{O}(\alpha_s))}{(p_{T,\text{jet}}^v)^2} - \frac{3(1 + \mathcal{O}(\alpha_s))}{(p_{T,\text{jet}}^{\text{ref}})^2} \right)^{-1},$$

3. Define

$$\Delta^{\text{ref}} \equiv \Delta(p_{T,\text{jet}}^{\text{ref}}, m_t, \alpha_s, \Lambda_{\text{QCD}}), \quad \Delta^v(p_{T,\text{jet}}^v - p_{T,\text{jet}}^{\text{ref}}, m_t, \alpha_s, \Lambda_{\text{QCD}}) \equiv \Delta(p_{T,\text{jet}}^v, m_t, \alpha_s, \Lambda_{\text{QCD}}) - \Delta^{\text{ref}}$$

4. Solve for ρ :

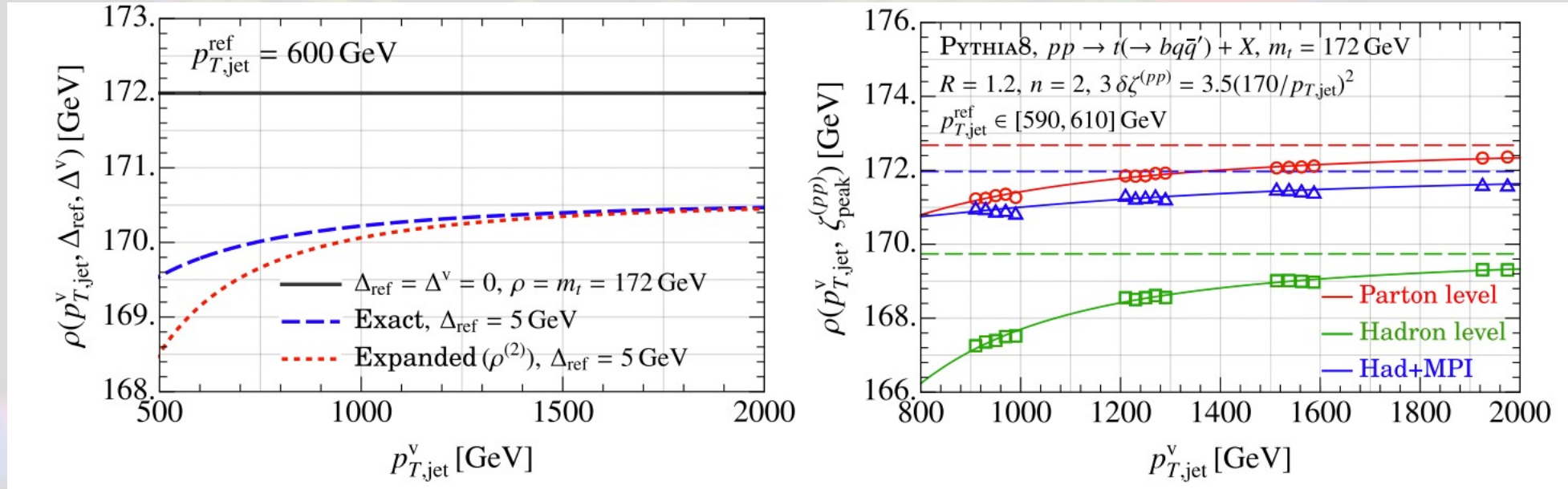
$$\rho(p_{T,\text{jet}}^v, \Delta^{\text{ref}}, \Delta^v) = \sqrt{F_{\text{pert}}} \frac{p_{T,\text{jet}}^{\text{ref}}}{p_{T,\text{jet}}^{\text{ref}} + \Delta^{\text{ref}}} \left(1 - \frac{2p_{T,\text{jet}}^{\text{ref}} \Delta^{\text{ref}} + (\Delta^{\text{ref}})^2}{2(p_{T,\text{jet}}^v)^2} + \frac{(p_{T,\text{jet}}^{\text{ref}} + \Delta^{\text{ref}})^2 (\Delta^{\text{ref}} + \Delta^v)}{8(p_{T,\text{jet}}^v)^3} + \mathcal{O}\left(\frac{1}{(p_{T,\text{jet}}^v)^4}\right) \right)$$

5. The asymptotic value for $p_{T,\text{jet}}^v$ depends only on m_t and Δ^{ref} .

Supplementary material

Fit function:

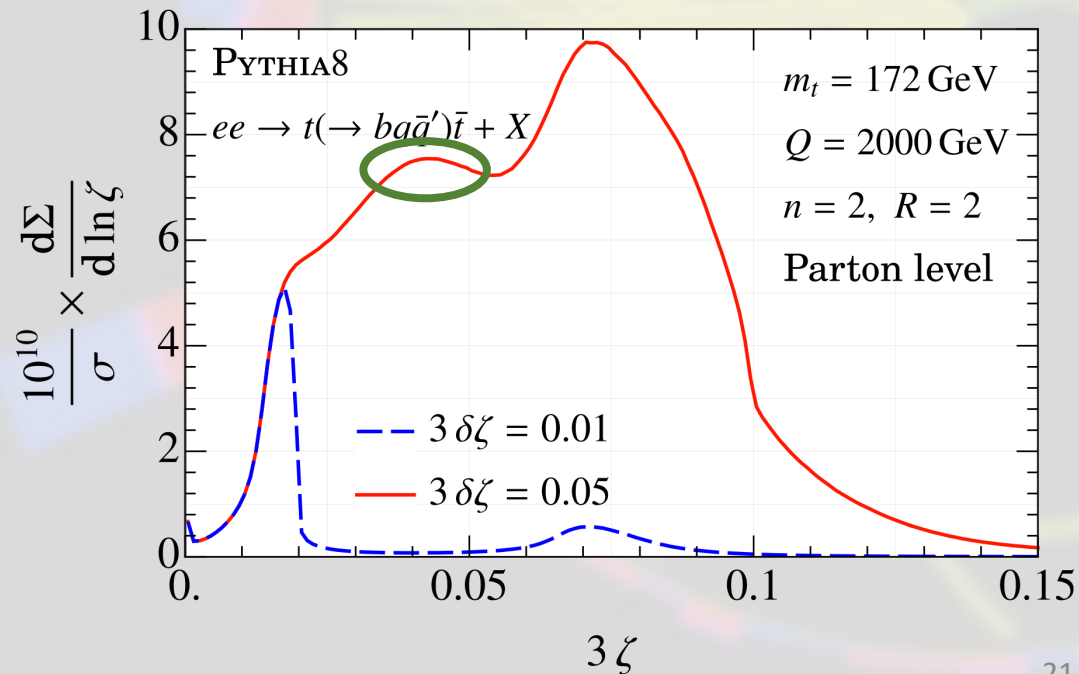
$$\rho = \rho_{\text{asy}} + c_2(p_{T,\text{jet}}^{\text{v}})^{-2} + c_3(p_{T,\text{jet}}^{\text{v}})^{-3}$$



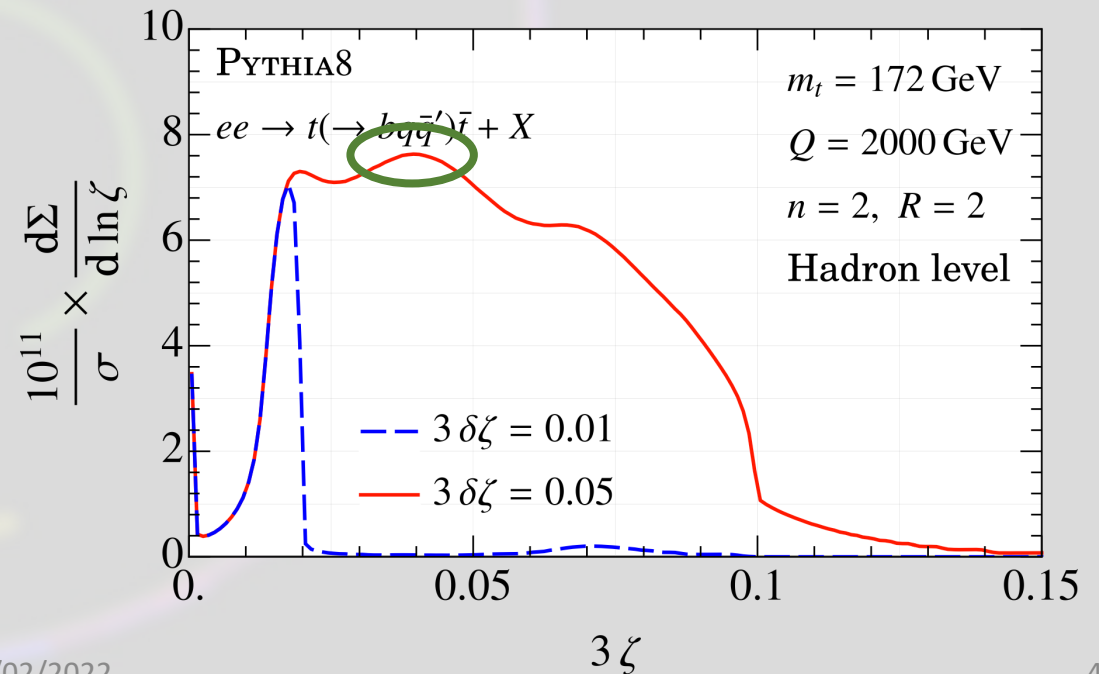
Further improved?

Using the equatorial configuration we projected onto the top peak. However the W also imprints on the correlator in a different part of the parameter space.

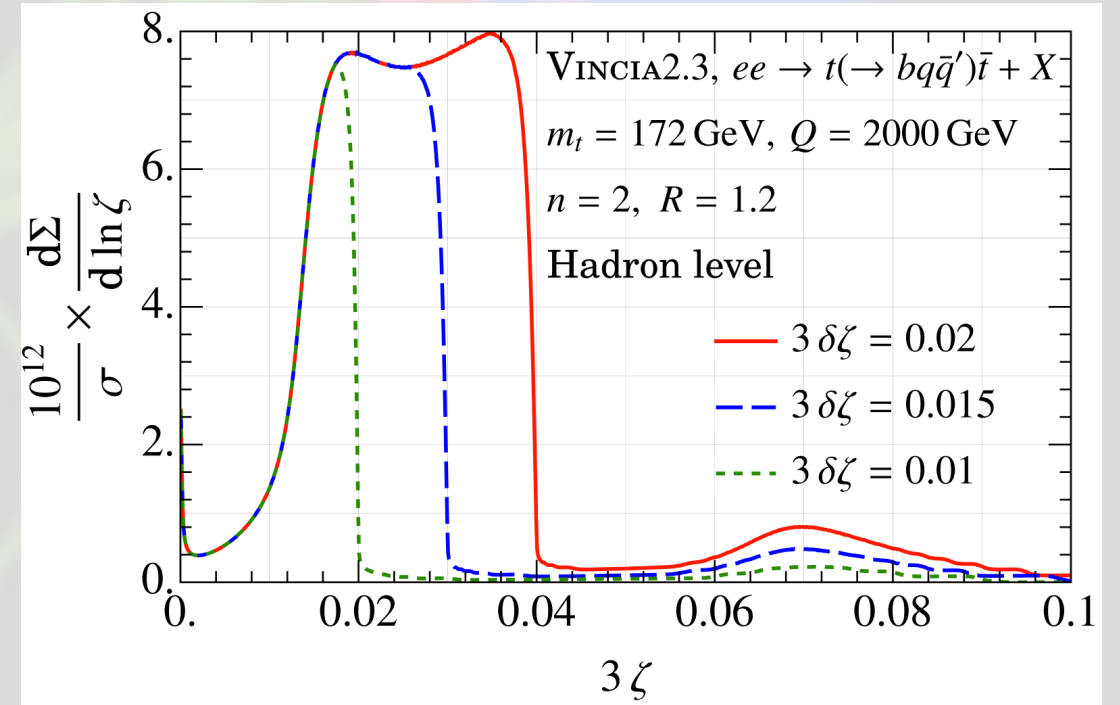
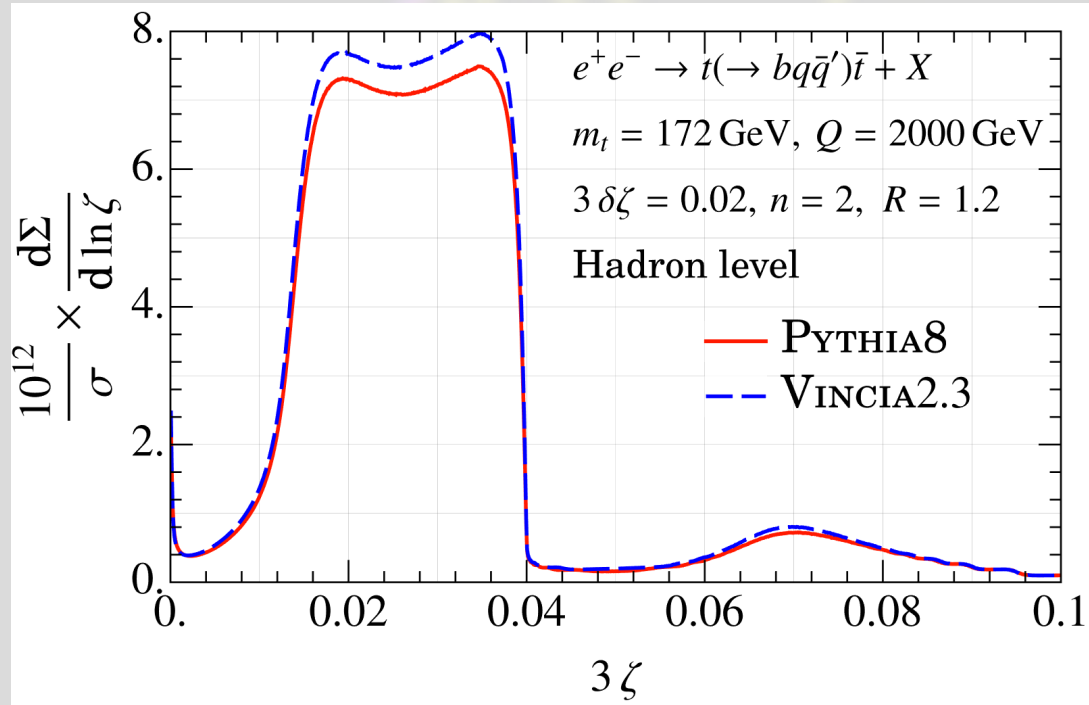
The distribution $\frac{d\Sigma(\delta\zeta)}{d\zeta_W d\zeta}$ is independent of the pt distribution, gives $m_t(m_W)$.



21/02/2022

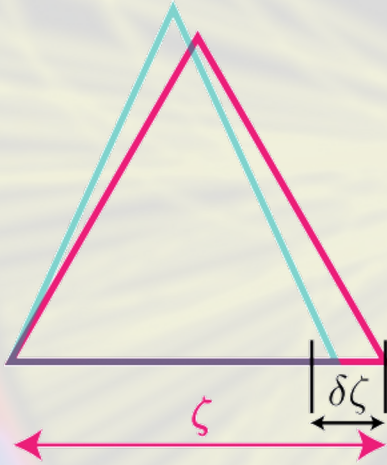


Supplementary material

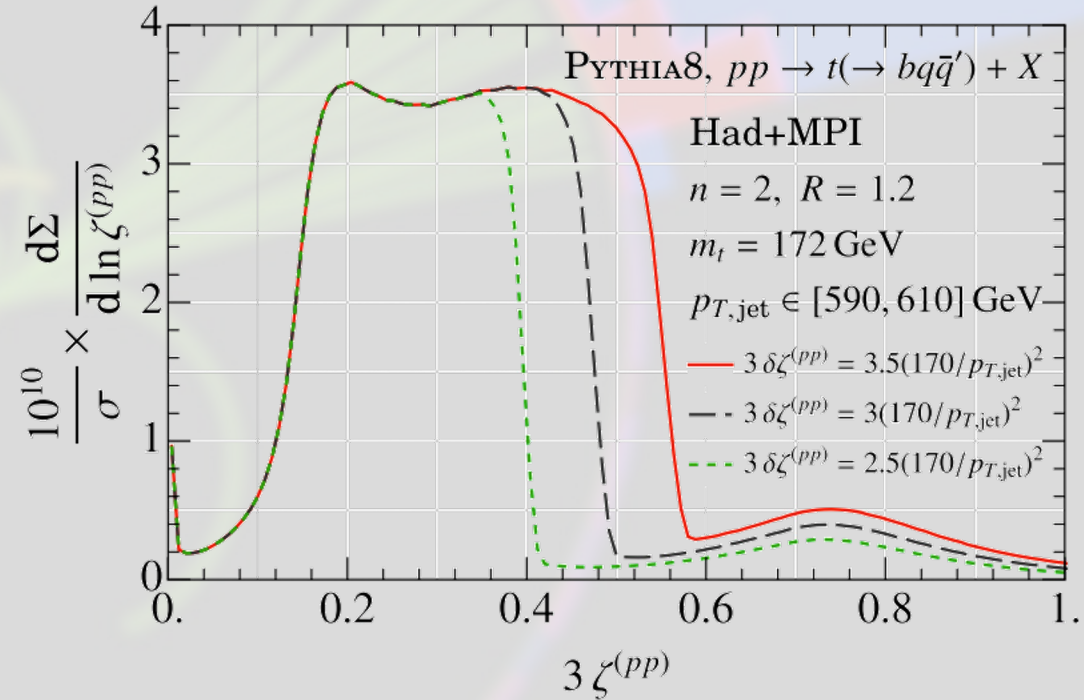


Supplementary material

Asymmetry cut $\delta\zeta$ only constrains triangles with $\zeta > 2\delta\zeta$

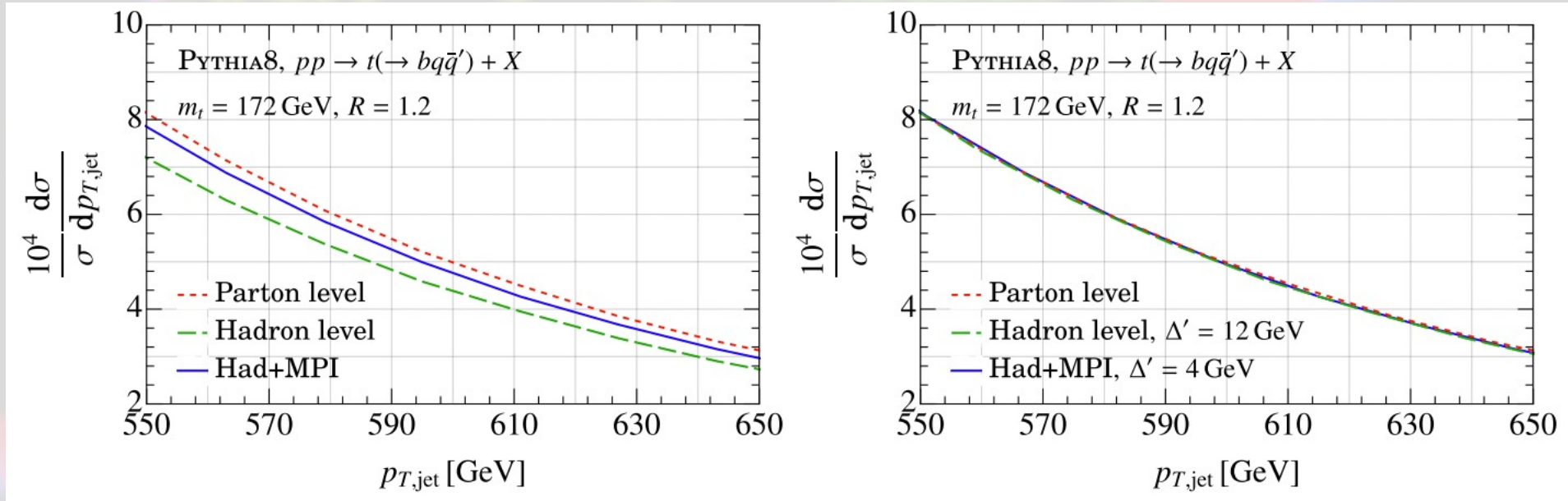


$$\frac{d\Sigma}{d\zeta} \approx 4(\delta\zeta)^2 G^{(n)}(\zeta, \zeta, \zeta; m_t), \quad \delta\zeta \ll \zeta$$

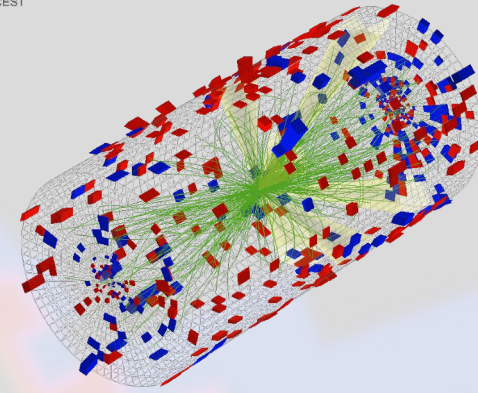


Supplementary material

Here we show $p_{T,\text{jet}}$ shifts relative to parton level:



Correlation Functions



- Case study from study of the QGP in Pb-Pb:

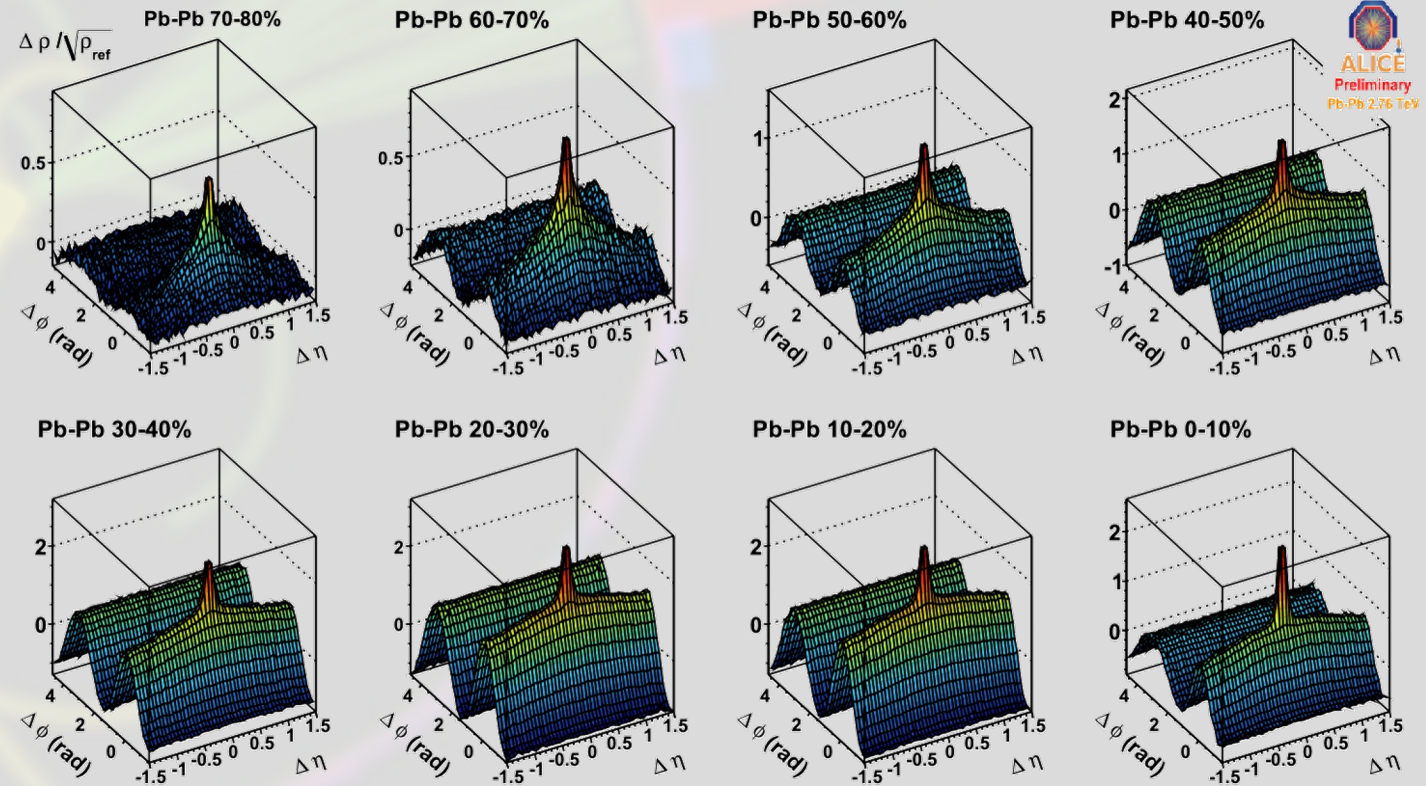
$$\langle N(\eta_1, \phi_1) N(\eta_2, \phi_2) \rangle = N_1 N_2 P(\eta_1, \phi_1, \eta_2, \phi_2)$$

$$\sim \sum_X N_X(\eta_1, \phi_1) N_X(\eta_2, \phi_2) \langle \text{Pb} - \text{Pb} | X \rangle \langle X | \text{Pb} - \text{Pb} \rangle$$

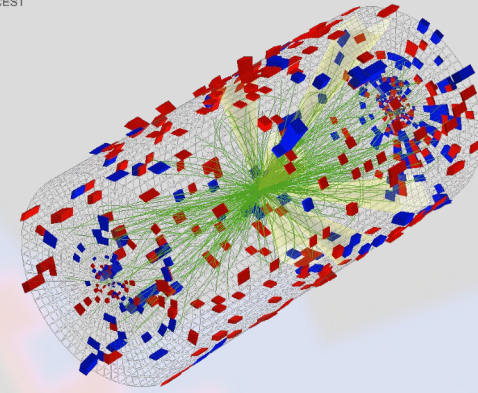
$$= \sum_X \langle \text{Pb} - \text{Pb} | \hat{N}(\eta_1, \phi_1) \hat{N}(\eta_2, \phi_2) | X \rangle \langle X | \text{Pb} - \text{Pb} \rangle$$

$$= \langle \text{Pb} - \text{Pb} | \hat{N}(\eta_1, \phi_1) \hat{N}(\eta_2, \phi_2) | \text{Pb} - \text{Pb} \rangle$$

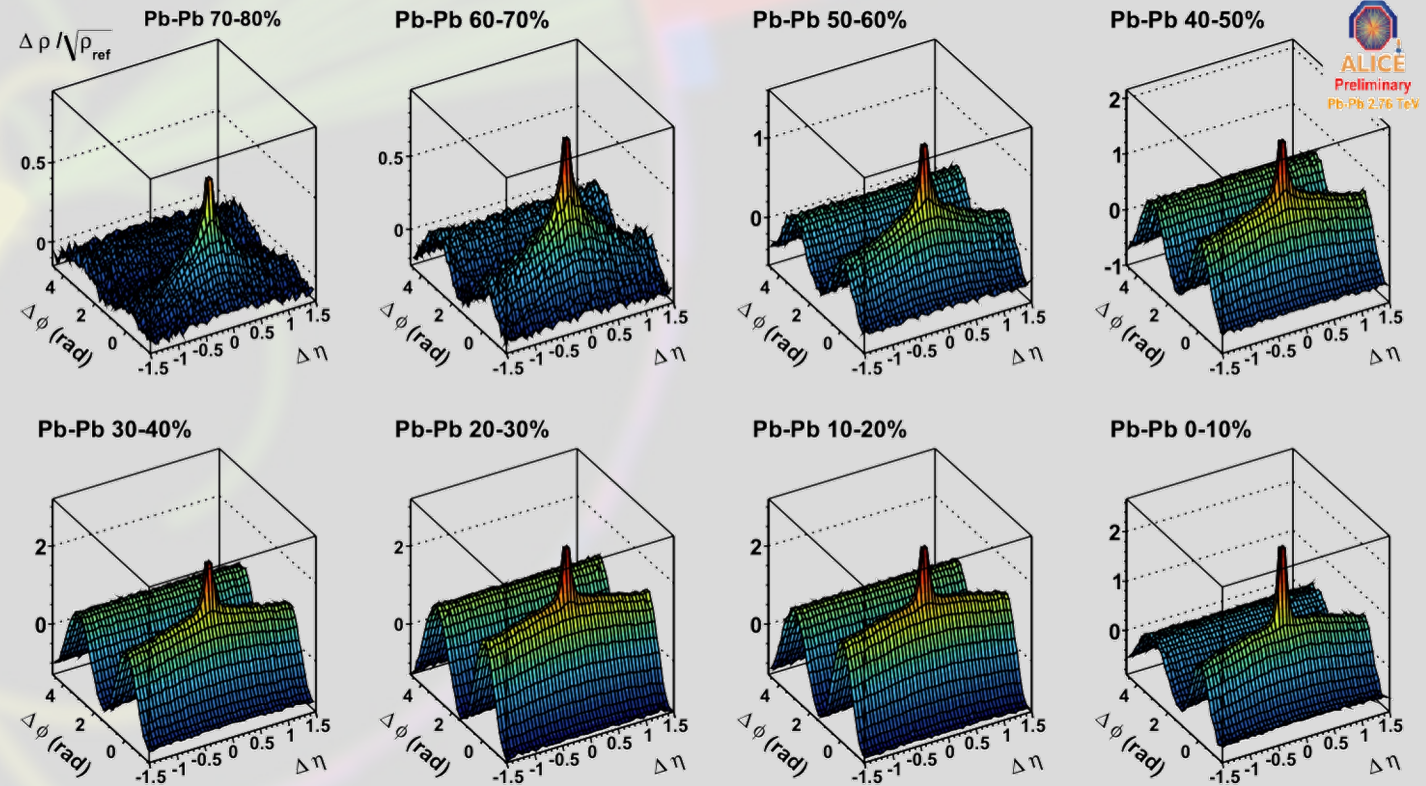
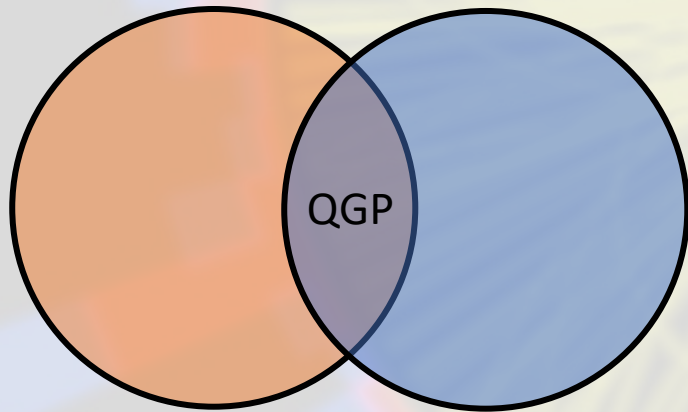
$$\frac{dN}{d^2 p d^2 k d\eta d\xi} = \langle \hat{\sigma}(k) \hat{\sigma}(p) \rangle_{P,T}$$



Correlation Functions

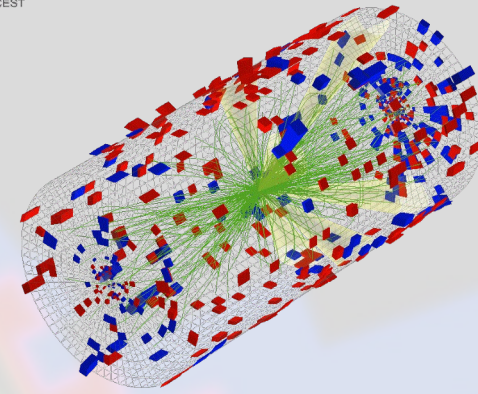


- Case study from study of the QGP in Pb-Pb:

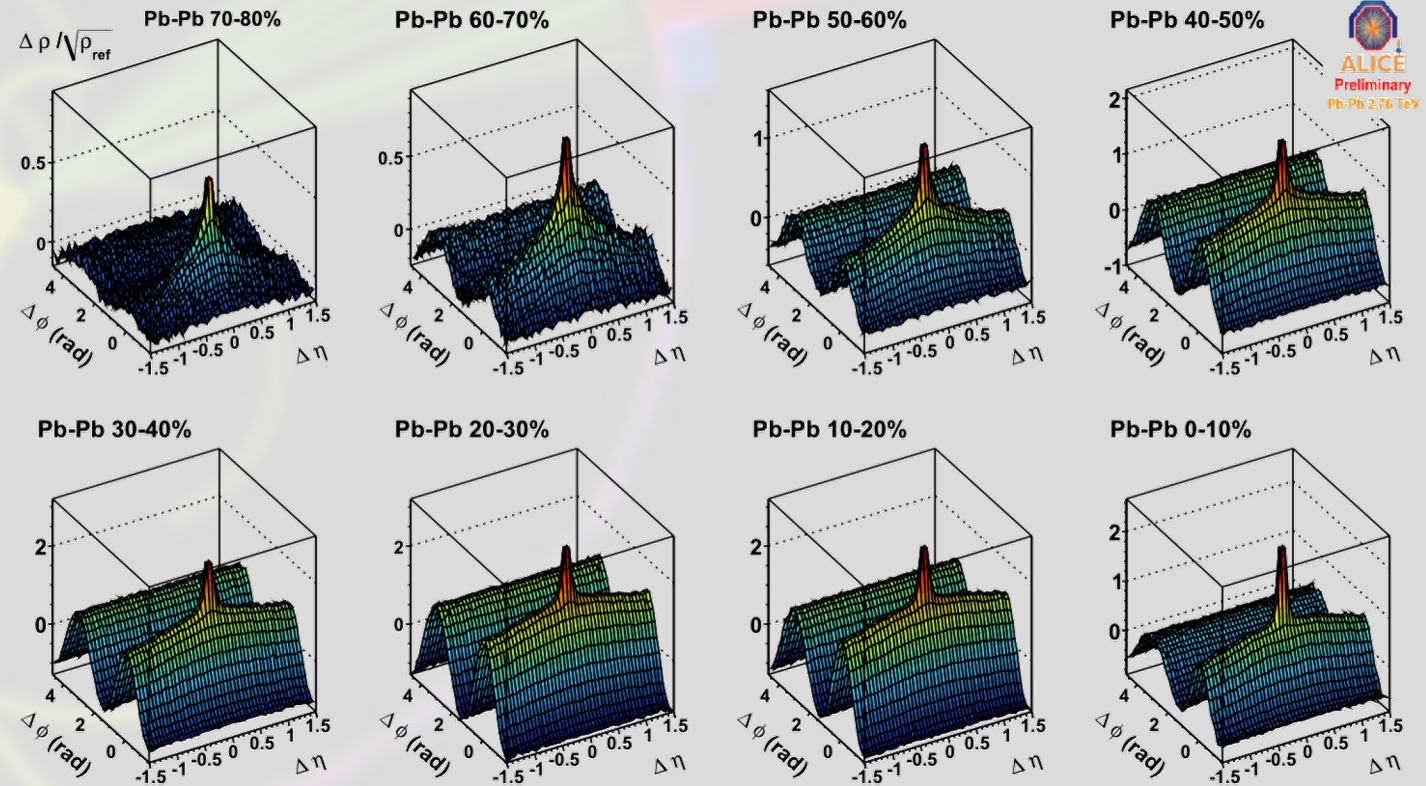
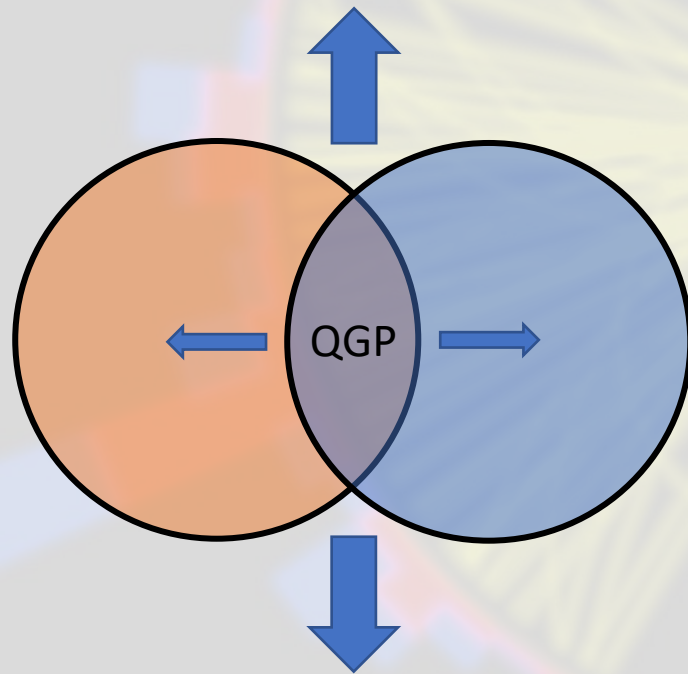


[1106.6057](https://doi.org/10.1106.6057)

Correlation Functions

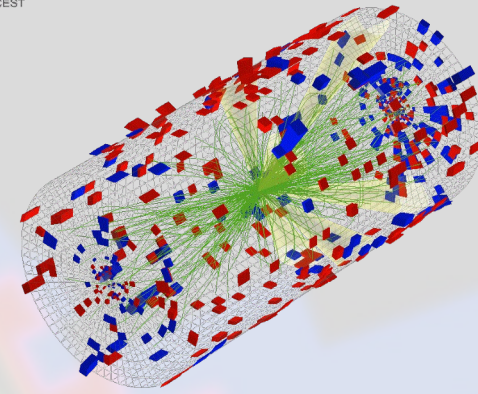


- Case study from study of the QGP in Pb-Pb:

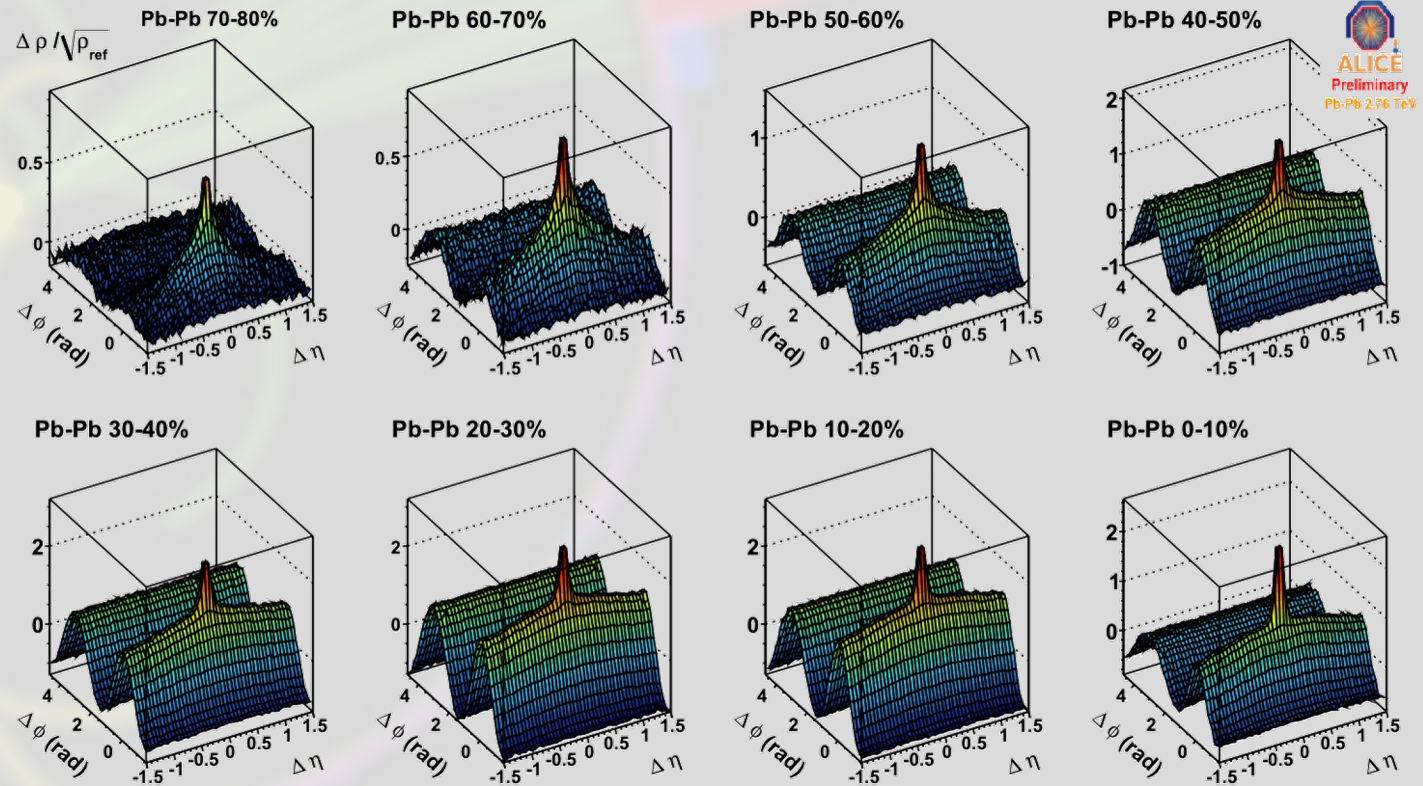
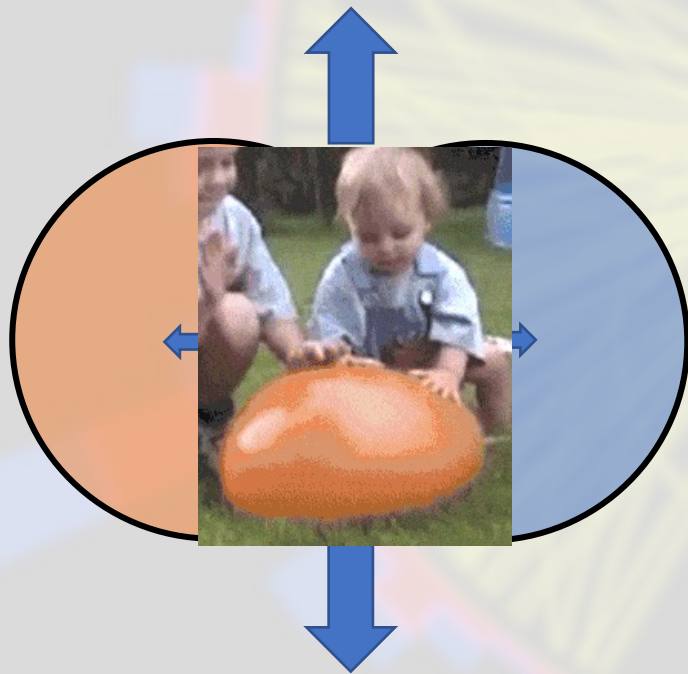


[1106.6057](https://doi.org/10.1106.6057)

Correlation Functions

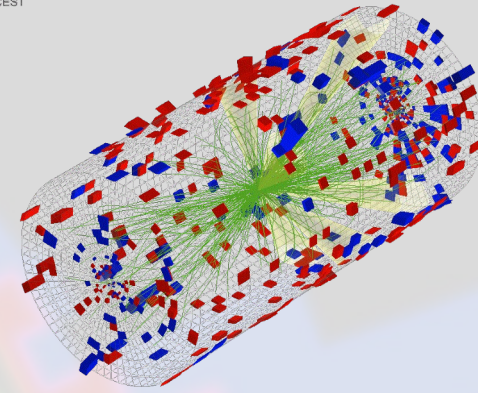


- Case study from study of the QGP in Pb-Pb:

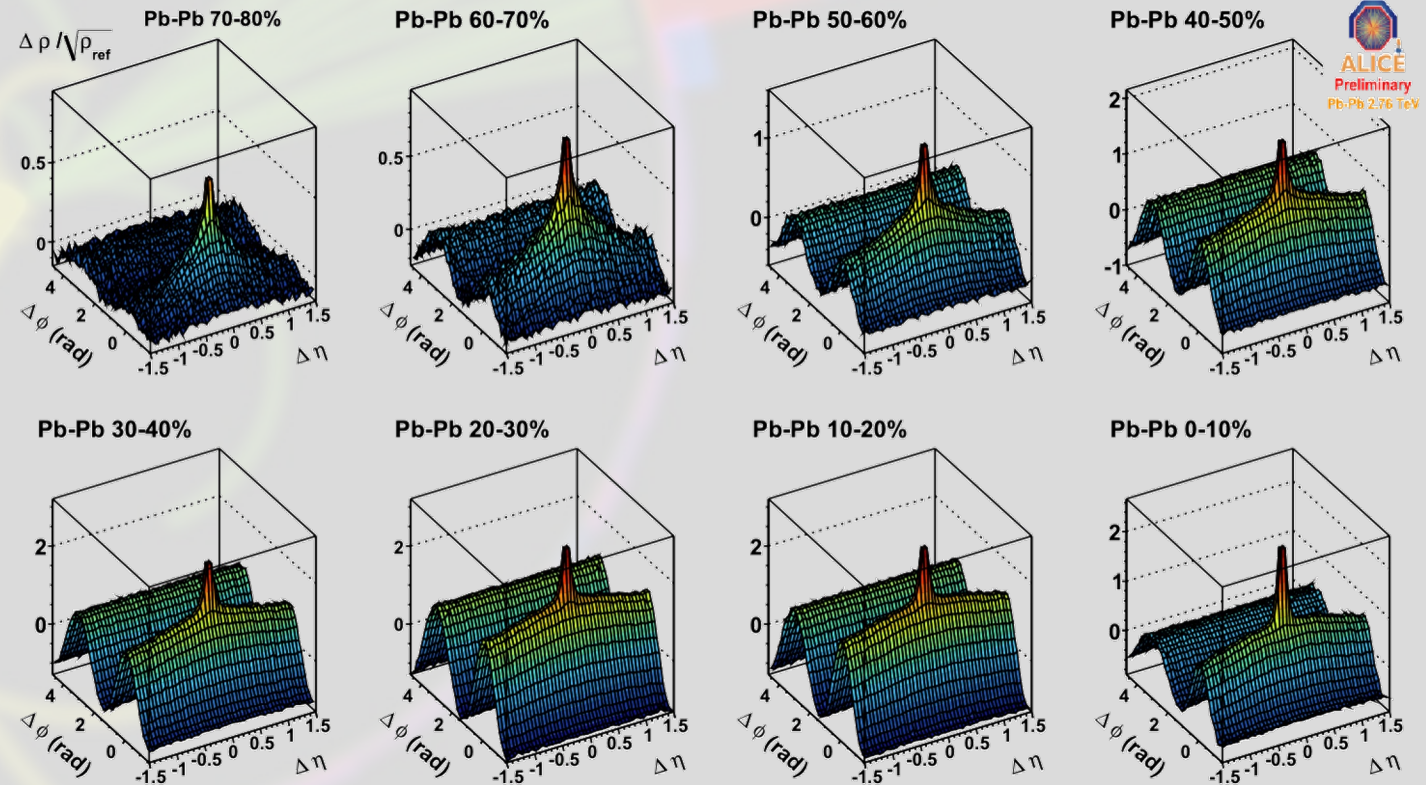
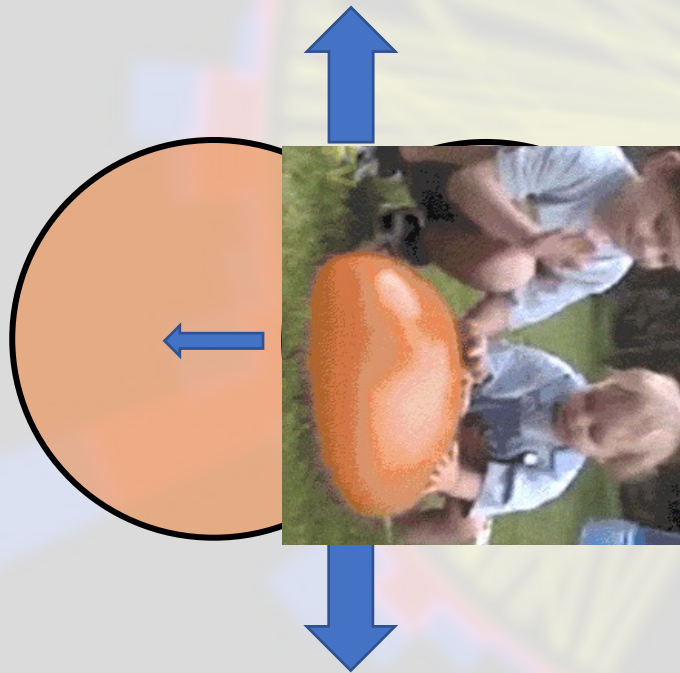


[1106.6057](https://doi.org/10.1106.6057)

Correlation Functions



- Case study from study of the QGP in Pb-Pb:



[1106.6057](https://doi.org/10.1146/annurev-nucl-102011-125212)

Correlation Functions

$$\mathcal{E}(\vec{n}) = \lim_{r \rightarrow \infty} \int_0^{\infty} dt r^2 n^i T_{0i}(t, r\vec{n})$$

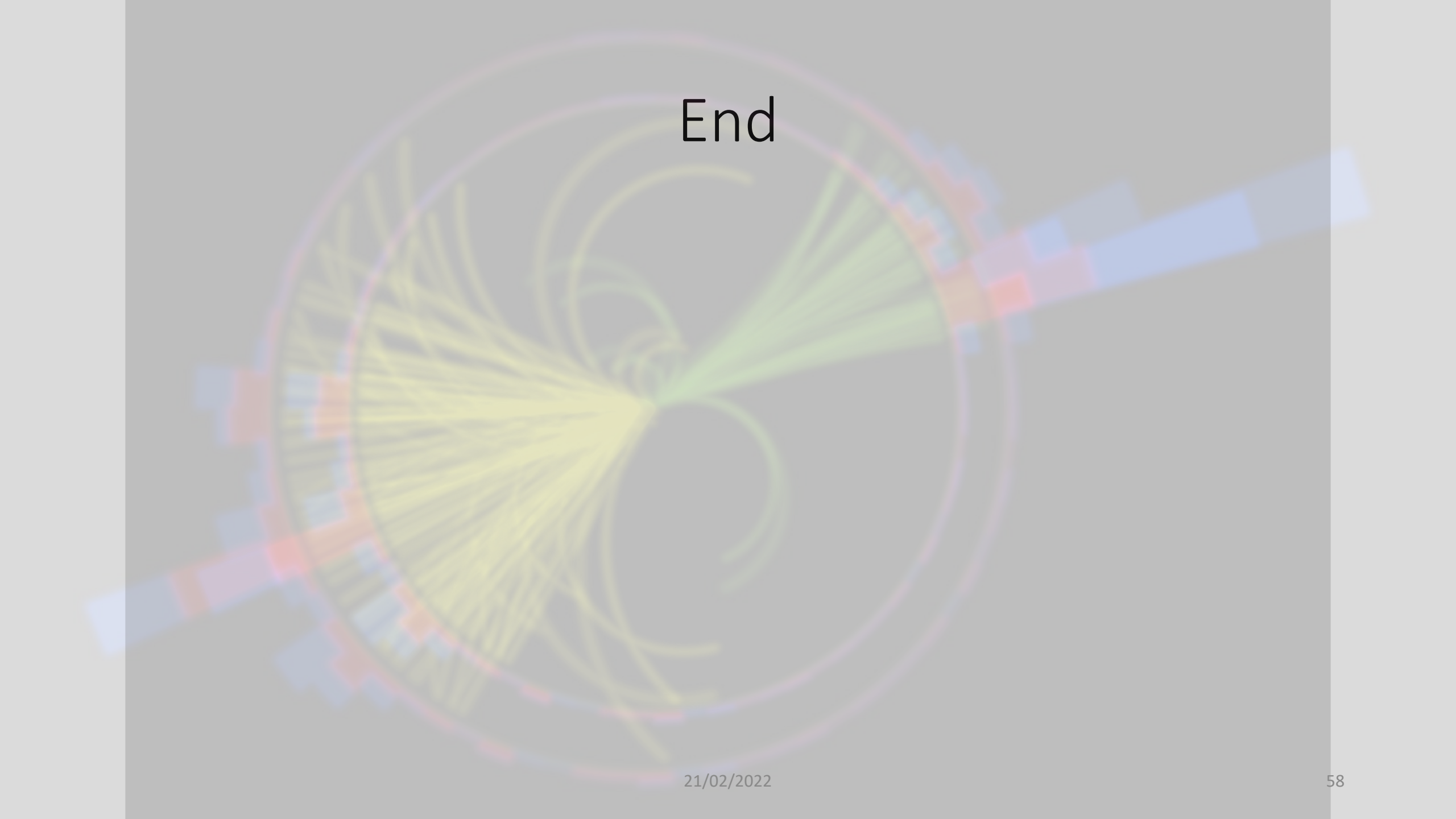
$\langle \mathcal{E}(\vec{n}_1) \mathcal{E}(\vec{n}_2) \rangle \leftarrow$ Not the QFT VEV.

Quantum mechanical expectation value, just as $\langle \psi | \hat{p} | \psi \rangle = \langle p \rangle$:

i.e.

$$\delta_{i \rightarrow j} = \langle j | i \rangle \quad \text{let } |j\rangle = \mathcal{O} | \Omega \rangle$$

$$\langle \mathcal{E}(\vec{n}_1) \mathcal{E}(\vec{n}_2) \rangle = N \langle \Omega | \mathcal{O}^\dagger \hat{\mathcal{E}}(\vec{n}_1) \hat{\mathcal{E}}(\vec{n}_2) \mathcal{O} | \Omega \rangle$$

A complex network diagram is centered on the page. It features a central node from which numerous lines radiate outwards. The lines are color-coded: a large, dense fan of yellow lines extends to the left, while a smaller fan of light green lines extends to the right. The network also includes several curved lines and segments of different colors (blue, red, orange, purple) that form a circular structure around the central node. The entire diagram is overlaid on a light gray background.

End